© 2021. Published by The Company of Biologists Ltd | Development (2022) 149, dev199916. doi:10.1242/dev.199916

STEM CELLS AND REGENERATION

RESEARCH ARTICLE

Toll signalling promotes blastema cell proliferation during cricket leg regeneration via insect macrophages

Tetsuya Bando[1,], Misa Okumura[1], Yuki Bando[2], Marou Hagiwara[2], Yoshimasa Hamada[1,*], Yoshiyasu Ishimaru[3], Taro Mito[3], Eri Kawaguchi[4,‡], Takeshi Inoue[4,§], Kiyokazu Agata[4,¶], Sumihare Noji[3] and Hideyo Ohuchi[1,**]**

ABSTRACT

Hemimetabolous insects, such as the two-spotted cricket *Gryllus bimaculatus*, can recover lost tissues, in contrast to the limited regenerative abilities of human tissues. Following cricket leg amputation, the wound surface is covered by the wound epidermis, and plasmatocytes, which are insect macrophages, accumulate in the wound region. Here, we studied the function of Toll-related molecules identified by comparative RNA sequencing during leg regeneration. Of the 11 Toll genes in the *Gryllus* genome, expression of *Toll2-1*, *Toll2-2* and *Toll2-5* was upregulated during regeneration. RNA interference (RNAi) of *Toll*, *Toll2-1*, *Toll2-2*, *Toll2-3* or *Toll2-4* produced regeneration defects in more than 50% of crickets. RNAi of *Toll2-2* led to a decrease in the ratio of S- and M-phase cells, reduced expression of JAK/STAT signalling genes, and reduced accumulation of plasmatocytes in the blastema. Depletion of plasmatocytes in crickets using clodronate also produced regeneration defects, as well as fewer proliferating cells in the regenerating legs. Plasmatocyte depletion also downregulated the expression of Toll and JAK/STAT signalling genes in the regenerating legs. These results suggest that Spz-Toll-related signalling in plasmatocytes promotes leg regeneration through blastema cell proliferation by regulating the Upd-JAK/STAT signalling pathway.

KEY WORDS: Regeneration, Toll-related signalling, JAK/STAT signalling, Macrophages, Blastema, *Gryllus bimaculatus*

[1]Department of Cytology and Histology, Okayama University Graduate School of Medicine, Dentistry and Pharmaceutical Sciences, 2-5-1, Shikata-cho, Kita-ku, Okayama city, Okayama 700-8558, Japan. [2]Faculty of Medicine, Okayama University Medical School, 2-5-1, Shikata-cho, Kita-ku, Okayama city, Okayama 700-8558, Japan. [3]Division of Bioscience and Bioindustry, Graduate School of Technology, Industrial and Social Sciences, Tokushima University, 2-1 Minami-Josanjima-cho, Tokushima City, Tokushima 770-8513, Japan. [4]Division of Biological Science, Graduate School of Science, Kyoto University, Kitashirakawa-Oiwake, Sakyo, Kyoto 606-8502, Japan.
*Present address: Division of Molecular Biology, Institute for Genome Research, Tokushima University, 3-18-15 Kuramoto-cho, Tokushima City, Tokushima 770-8503, Japan. ‡Present address: Center for iPS Cell Research and Application, Kyoto University, 53 Kawahara-cho, Shogoin, Sakyo-ku, Kyoto 606-8507, Japan. §Present address: Division of Adaptation Physiology, Faculty of Medicine, Tottori University, 86 Nishi-cho, Yonago 683-8503, Japan. ¶Present address: National Institute for Basic Biology, Nishigonaka 38, Myodaiji, Okazaki, Aichi 444-8585, Japan.

**Authors for correspondence (tbando@cc.okayama-u.ac.jp; ohuchi-hideyo@okayama-u.ac.jp)

T.B., 0000-0002-3038-7782; Y.I., 0000-0001-5668-9685; T.M., 0000-0002-3574-972X; T.I., 0000-0003-3289-4478; K.A., 0000-0002-5195-2576; S.N., 0000-0003-4441-1672; H.O., 0000-0003-1961-606X

Handling Editor: Steve Wilson
Received 18 June 2021; Accepted 28 September 2021

INTRODUCTION

Tissue regeneration allows the restoration of lost tissues from cells. Various animals, including planarians, insects, fishes, newts and frogs, have regenerative abilities. The regenerative abilities of amniotes, including chicks, mice and humans, are limited (Agata and Inoue, 2012). One crucial difference between regenerative and non-regenerative animals is the ability to form a blastema, a population of stem cells or dedifferentiated cells that proliferate and differentiate into several types of cells to restore the lost tissue, although some species, such as hydra, do not require blastema formation for regeneration (Agata et al., 2007; Vogg et al., 2019). A key goal in the field of regenerative biology is to identify the factors that trigger blastema formation, which is an initial step in tissue regeneration.

Following tissue injury, a defence response occurs around the wound site. Neutrophils and macrophages expressing proinflammatory genes migrate to the wound region to eliminate infectious microbes and clear debris from injured cells (Anders and Schaefer, 2014; Westman et al., 2020). These phagocytic cells also express pattern recognition receptors, such as Toll-like receptors (TLRs), to detect infectious microbes, and Janus kinase/Signal transducer and activator of transcription (JAK/STAT) signalling components, including interleukin receptors (IL-Rs), to receive cytokine (Hu et al., 2007). In vertebrates, infectious microbes are directly detected by TLRs (Kawai and Akira, 2011; Pandey et al., 2014; Szatmary, 2012). In insects, infectious microbes, such as gram-positive bacteria, yeasts and fungi, are mostly detected by Toll via proteoglycan recognition proteins (PGRPs) and clip-domain serine proteinases (clip-SPs), and gram-negative bacteria are detected by PGRP-LC and immune deficiency (Imd) signalling (Fig. S1) (Anthoney et al., 2018; Leulier and Lemaitre, 2008; Myllymäki et al., 2014). In both vertebrates and invertebrates, cytokines are received by IL-Rs and activate JAK/STAT signalling (Arbouzova and Zeidler, 2006).

Recent studies have shown that macrophages promote tissue regeneration in axolotl and zebrafish (Godwin et al., 2013; Petrie et al., 2014). Phagocytic uptake of liposome-encapsulated clodronate (Clo-lipo) is a well-established method for depleting macrophages, as liposome is specifically incorporated into phagocytes. Clodronate induces apoptosis by antagonising ATP metabolism (Van Rooijen and Sanders, 1994). In one study, macrophage-depleted axolotls (*Ambystoma mexicanum*) treated with Clo-lipo did not regenerate the amputated portions of limbs caused by downregulation of blastema marker genes, whereas regeneration was successful in control axolotls treated with PBS-lipo (Godwin et al., 2013). Axolotl macrophages respond to pathogen-associated molecular patterns (PAMPs) and damage-associated molecular patterns (DAMPs) via TLRs (Debuque et al., 2021). In zebrafish, macrophages infiltrate the affected area to engulf cellular debris (Li et al., 2012), and maintain appropriate levels of

Development (2022) 149, dev199916. doi:10.1242/dev.199916

inflammation to induce expression of regeneration-promoting genes (Hasegawa et al., 2017). Thus, macrophage-depleted transgenic zebrafish exhibit altered fin regeneration, likely mediated by a reduction in blastema cell proliferation (Petrie et al., 2014). In earthworms, which are regenerative invertebrates, depletion of phagocytic cells impairs tissue regeneration (Bodó et al., 2021). Macrophages promote cell proliferation, even in partially regenerative vertebrates such as *Xenopus* froglets or mice. When a portion of a limb is amputated in these species, a cartilaginous callus is formed by proliferation of chondrocytes. However, Clo-lipo treatment of either species inhibits callus formation (Miura et al., 2015). Hence, the efficient functioning of macrophages is not sufficient, but is required, for regeneration. The precise signalling pathways that function in phagocytic cells during regeneration remain unclear.

Insects have an open blood-vascular system and their body fluids contain several types of haemocytes, including prohaemocytes, phagocytes and non-phagocytic cells (Hillyer, 2016). Prohaemocytes are the stem cells of other haemocytes. Plasmatocytes and granulocytes of *Lepidoptera* and plasmatocytes of *Drosophila* are the primary phagocytic and encapsulating cells involved in defence responses, and are analogous to mammalian macrophages (Browne et al., 2013; Evans et al., 2003; Ribeiro and Brehélin, 2006). Depletion of phagocytic cells using clodronate has also been achieved in mosquitoes and fruit flies (Kumar et al., 2021; Kwon and Smith, 2019).

To investigate the molecular link between insect immunity (Hillyer, 2016) (Fig. S1) and blastema formation during tissue regeneration, we focused on the role of Toll signalling pathways and plasmatocytes during leg regeneration of a hemimetabolous insect, because its regenerative abilities are greater than those of holometabolous insects. The two-spotted cricket *Gryllus bimaculatus* can restore the lost part of an amputated leg in the nymphal stage (Bando et al., 2017; Mito and Noji, 2008). When we amputated a cricket leg at the tibia, the wound surface was covered by a scab and wound epidermis (Mito et al., 2002). Prior studies have demonstrated that the formation of a blastema (Mito et al., 2002; Nakamura et al., 2008a) occurs through cell proliferation processes regulated by the JAK/STAT and Hippo signalling pathways (Bando et al., 2009, 2013). The lost part of the leg is recognised depending on positional information along the proximodistal axis, mediated by Dachsous/Fat protocadherins (Bando et al., 2009, 2011a, b). This is followed by redifferentiation of blastema cells. During repatterning, leg-patterning genes are re-expressed in the blastema (Ishimaru et al., 2015; Nakamura et al., 2008b) via an epigenetic mechanism (Hamada et al., 2015). In *G. bimaculatus*, as in other insects, two out of the six types of haemocytes – plasmatocytes and granulocytes – have been reported to respond to infection (Cho and Cho, 2019; Sokolova et al., 2000). The plasmatocytes are insect macrophages; however, the molecular link between immunity and the plasmatocytes is still unclear, although it may involve JAK/STAT and Toll signalling pathways.

In this study, the expression of Toll signalling genes was altered during leg regeneration in *G. bimaculatus*. RNA interference (RNAi) of Toll family genes resulted in defective regeneration and impaired regeneration phenotypes, indicating that Toll signalling promotes leg regeneration. RNAi of *Toll2-2* resulted in downregulated expression of JAK/STAT signalling components and decreased cell proliferation in the blastemas of regenerating legs. We also analysed the role of plasmatocytes, because *Toll2-2* is expressed in plasmatocytes. Depletion of plasmatocytes in crickets resulted in decreased cell proliferation in the blastema and failure of leg regeneration. These findings suggest that *Toll2-2*-expressing plasmatocytes activate blastema cell proliferation, promoting leg regeneration via Toll signalling.

RESULTS

Comparative RNA sequencing (RNA-seq) analysis reveals upregulation of immune-related gene expression in regenerating legs

To identify signalling pathways activated in early regeneration processes, RNA-seq analysis was performed and gene expression between regenerating legs at an early phase [3 hours post-amputation (hpa)] and in non-regenerating legs (0 hpa) was compared. All reads obtained from early regenerating legs (RLs) and non-regenerating legs (NLs) were assembled into contigs and each read from RLs and NLs was mapped to the contigs to calculate the reads per kilobase of exons per million reads (RPKM) value. Comparison of RPKM values of each contig (Table S1) indicated that 908 contigs were only expressed in the RLs, and the expression of 2565 contigs was upregulated more than twofold in the RLs (Table 1). To exclude genes expressed at a low level, we omitted contigs for which read counts were <10 and RPKM values were <5, resulting in 59 contigs only expressed in the RLs and 957 contigs upregulated in the RLs being selected for further analyses. To obtain an overview of these contigs, 32 out of 59 and 549 out of 957 contigs, annotated using the BLASTX program (Table S2), were analysed using Blast2GO software. Gene ontology (GO) terms relating to biological processes, molecular functions and cellular components with which more than six contigs were annotated are summarised in Fig. 1 and Fig. S2A. Notably, transcripts related to ‘antimicrobial humoral response’ and ‘haemocyte migration’ in the biological process category were upregulated in the RL group compared with the NL group. These GO terms were not identified in our previous RNA-seq analyses at 24 hpa (Bando et al., 2013). In contrast, GO terms that were upregulated in the 24 hpa RL (Bando et al., 2013), such as ‘cell differentiation’ and ‘cell death’ in biological processes, were not upregulated in the 3 hpa RL (Fig. 1).

We identified transcripts encoding signalling pathway components that were upregulated in the RL (Fig. S2B). Transcripts encoding components related to vascular endothelial growth factor, insulin-like growth factor, fibroblast growth factor, transforming growth factor-beta (TGFβ), Wnt and Toll signalling pathways were upregulated in the RL group compared with the NL group. Previous studies have demonstrated the involvement of JAK/STAT (Bando et al., 2013), TGFβ and Wnt (Ishimaru et al., 2018; Mito et al., 2002; Nakamura et al., 2007), and Notch (Bando et al., 2011b) signalling pathways during cricket leg regeneration. We focused on the Toll signalling pathway in this study, because the function of Toll signalling during regeneration is unclear.

Expression of Toll-related genes is activated by amputation to promote leg regeneration

Eleven Toll genes from the *Gryllus* genome have been identified (Ylla et al., 2021) and designated *Toll*, *Toll2-1-5*, *Toll6-1-2*, *Toll7*, *Toll8* and *Toll9*, based on amino acid homology with other insect orthologues (Hillyer, 2016) (Fig. 2A, Fig. S3). Five paralogues, Toll2-1 to Toll2-5, are phylogenetically close to termite *Zootermopsis nevadensis* Toll-like receptor 2, but not close to *Drosophila* Toll-2; *Drosophila* Toll-2 was close to Toll-7 (Fig. 2A). We cloned cDNA fragments of all *Gryllus* Toll genes from cDNA obtained from RLs. In the RNA-seq analysis, expression of *Toll2-5*, *Toll8* and *Toll2-2* were upregulated in RLs (Fig. S2B). Quantitative PCR (qPCR) examination of temporal expression changes in the *Gryllus* Toll genes revealed more than twofold upregulated expression of *Toll2-1*, *Toll2-2* and *Toll2-5* in RLs at 3, 24 and 48 hpa compared with RLs at 0 hpa (Fig. 2B). In particular, the expression of *Toll2-1* and *Toll2-2* was upregulated more than 3-fold

Development (2022) 149, dev199916. doi:10.1242/dev.199916

Table 1. Process of short reads assembly and annotation of assembled contigs

	Total length (bp)	Average length (bp)	Number of contigs	Number of contigs (number of reads ≥10, RPKM ≥5)	Number of BLASTed contigs
Assembled transcripts	14,368,694	2252	20,317	8441	
Only expressed in RLs			908	59	32
Upregulated in RLs			2565	957	549
Similarly expressed in both RLs and NLs			10,669	6116	
Downregulated in RLs			2797	1271	
Only expressed in NLs			1194	38	

and 5-fold, respectively, at 3 hpa. Their elevated expression was maintained at 24 hpa and slightly decreased at 48 hpa. Expression of *Toll2-5* was gradually upregulated from 3-fold to 10-fold from 3 to 48 hpa. Conversely, expression levels of *Toll2-4*, *Toll6-1*, *Toll6-2*, *Toll7*, *Toll8* and *Toll9* were reduced to less than 50% at certain time points during regeneration (Fig. 2B). Expression changes of *Toll* and *Toll2-3* were significant, but were upregulated to less than twofold (*Toll*) or downregulated more than 50% (*Toll2-3*) at 3, 24 and 48 hpa (Fig. 2B).

The observed changes in expression prompted us to examine further the involvement of the *Gryllus* Toll genes in leg regeneration. To identify regeneration-associated Toll genes, RNAi targeting each of the Toll genes was performed at the third instar. The morphologies of the RLs were compared with the morphologies of control legs at the fifth instar. Double-stranded RNA (dsRNA) targeting *DsRed* was used as a nonspecific control. We performed qPCR to estimate the reduction in mRNA levels of target genes in regenerating tibiae of RNAi crickets compared with those of *DsRed*^{RNAi} crickets at 48 hpa. RNAi against each Toll gene significantly reduced the transcript level to <50% of each control level (Fig. S4A), confirming the efficiency of RNAi.

Next, the phenotypes of RLs following RNAi targeting genes encoding Toll signalling molecules (Fig. 3B) at the fifth instar were determined and were categorised as class 1, class 2 and class 3 (Fig. 3A,C, Fig. 4). Class 3 was the normally regenerated leg found in the *DsRed*^{RNAi} crickets. In this class, the lost portion of the tibia was regrown, and tibial spurs were reconstructed at the distal end of the regrown tibia. The lost tarsus was reconstructed and segmented into tarsal segments 1 and 3 and the claws (Fig. 4). Class 2 was defined as an impaired regeneration phenotype. In this phenotype, the lost part of the tibia was not regrown, and tibial spurs were not reconstructed. The lost tarsus was reconstructed but was small and displayed an abnormal morphology. Class 1 was defined as a defective regeneration phenotype, in which no regeneration occurred, with no reconstruction of the lost tarsus (Fig. 3A, Fig. 4). In the RNAi experiments (Fig. 3C), >40% of crickets displayed class 1 phenotypes when RNAi targeted *Toll2-1* or *Toll2-2* (Fig. 3C). In addition, 18.8% and 32% of *Toll2-1*^{RNAi} and *Toll2-2*^{RNAi} crickets exhibited the class 2 phenotype, respectively; therefore, >70% of these RNAi crickets showed abnormalities during leg regeneration. These data, together with the observed expression changes during regeneration (Fig. 2B), indicate that *Toll2-1* and *Toll2-2* are important in leg regeneration.

To analyse further the role of Toll signalling, RNAi targeting ligands and intracellular component genes of the signalling (Fig. 3B) was performed. Whereas *Drosophila* has six *spz* paralogues (Viljakainen, 2015), we found two *spz* paralogues, which encode Toll ligands, in the *Gryllus* genome. Spz and Spz2 are paralogous to *Drosophila* Spz and Spz5, respectively. RNAi against *Gryllus spz* or *spz2* resulted in class 1 phenotypes occurring at rates of 21.1% and 16.7%, respectively (Fig. 3C,D), and those against *MyD88*, *tube*, *pelle* or *TRAF6*, which encode intracellular signalling molecules of Toll signalling (Fig. 3B), were 57.1%, 10.0%, 11.1% and 16.7%, respectively (Fig. 3C,D). The percentage of class 1 and class 2 phenotypes after *MyD88*^{RNAi} was 78.5%, which is comparable to that of *Toll2-1*^{RNAi} (75.1%) or *Toll2-2*^{RNAi} (72.0%) (Fig. 3C), suggesting that *Toll2-1* and *Toll2-2* may play crucial roles in leg regeneration via *MyD88*.

Next, we performed RNAi against *dorsal* (*dl*) and *Dorsal-related immunity factor* (*Dif*), both of which encode nuclear factor-kappa-B (NF-κB) transcription factors that function in the Toll signalling pathway (Fig. 3B) (Lindsay and Wasserman, 2014). Single RNAi against *dl* or *Dif* showed weak defects in leg regeneration. For example, 18.2% and 50.0% of *Dif*^{RNAi} cricket legs showed class 1

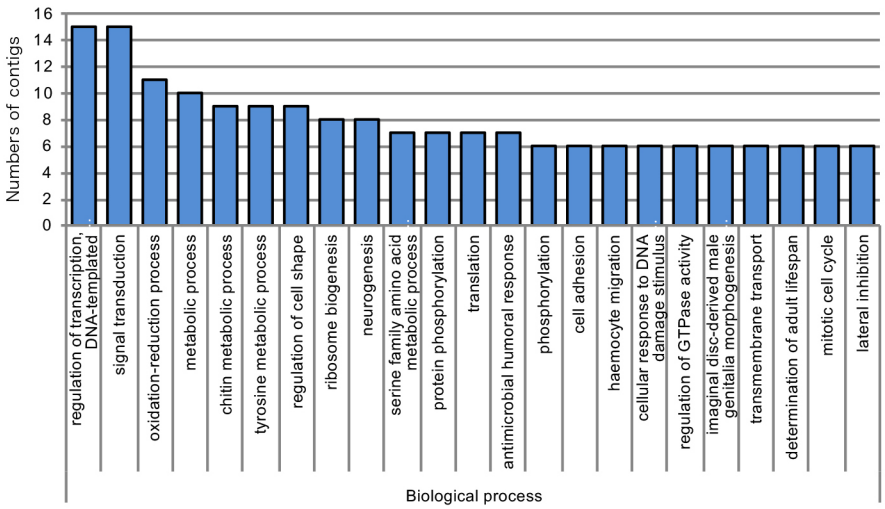

Fig. 1. Summary of RNA-seq results. Frequently counted gene ontology (GO) biological process terms by annotations of the transcripts with upregulated expression in RLs. The *y*-axis indicates the number of contigs.

Development (2022) 149, dev199916. doi:10.1242/dev.199916

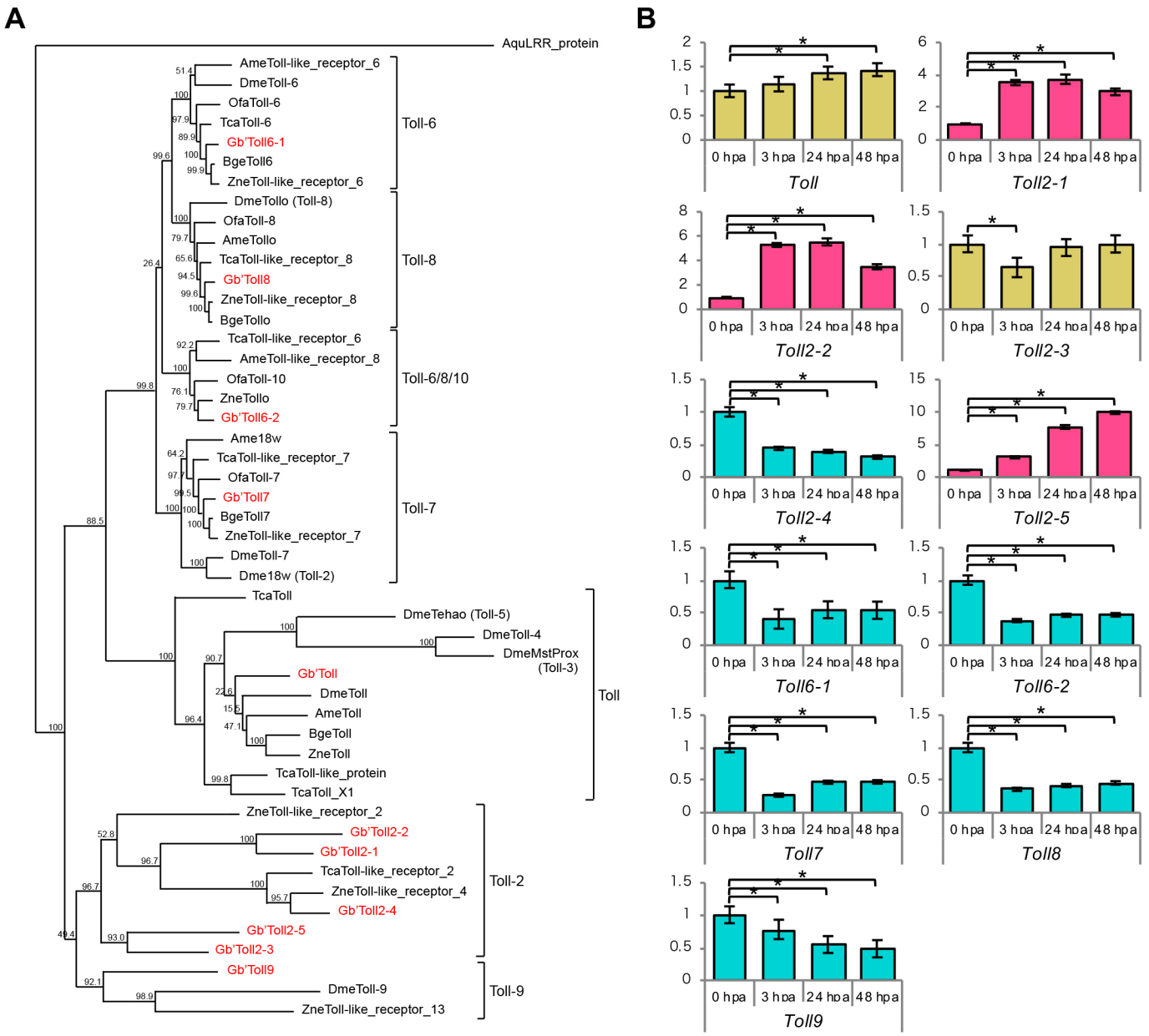

Fig. 2. Phylogenetic tree and temporal expression change of *Gryllus* Toll genes. (A) Phylogenetic tree of Toll genes of *Gryllus bimaculatus* and other insects based on the amino acid sequence alignment by CLUSTALW. Ame, *Apis mellifera*; Bge, *Blattella germanica*; Dme, *Drosophila melanogaster*; Gb, *Gryllus bimaculatus*; Ofa, *Oncopeltus fasciatus*; Tca, *Tribolium castaneum*; Zne, *Zootermopsis nevadensis*. Aqu (*Amphimedon queenslandica*) LRR was selected as an outgroup. (B) Temporal expression changes of *Gryllus* Toll genes at 0, 3, 24 and 48 hpa during leg regeneration. The *y*-axes show normalised expression at the 0 hpa and relative expression levels at 3, 24 and 48 hpa. **P*<0.05 (Tukey's test). *Toll2-1*, *Toll2-2* and *Toll2-5* (pink bars) were significantly upregulated and *Toll2-4*, *Toll6-1*, *Toll6-2*, *Toll7*, *Toll8* and *Toll9* (blue bars) were significantly downregulated at all time points. Genes for which expression changes were either less than twofold (*Toll*) or less than 50% (*Toll2-3*) are shown in yellow.

and 2 phenotypes, respectively (Fig. 3C,D). The proportion of the class 1 phenotype caused by *Dif*^{RNAi} was slightly increased in crickets with dual RNAi against *dl* and *Dif* (Fig. 3C). Given that Dl and Dif function downstream of both Toll and TNF signalling pathways (Igaki and Miura, 2014), we performed RNAi against *eiger* (*egr*) and *wengen* (*wgn*), which encode TNFα and TNF receptors, respectively. Leg regeneration occurred normally in *egr*^{RNAi} and *wgn*^{RNAi} crickets (Fig. S7A), despite the reduction of *egr* or *wgn* mRNA to approximately 10% compared with *DsRed*^{RNAi} controls (Fig. S7B). These RNAi results indicate that Spz and Spz2 could promote leg regeneration through Toll receptors, MyD88 and Dl/Dif dimers.

Because *Toll2-1*^{RNAi} and *Toll2-2*^{RNAi} crickets showed the most severe defects in leg regeneration (Fig. 3C), we quantified the mRNA levels of all *Gryllus* Toll genes in RLs of *Toll2-1*^{RNAi} and *Toll2-2*^{RNAi} crickets at 48 hpa (Fig. S5A,B). In the *Toll2-1*^{RNAi} RLs, the relative amount of *Toll2-2* mRNA was significantly decreased to 54%, whereas *Toll* and *Toll2-4* mRNAs were significantly increased to 160% and 152%, respectively (Fig. S5A). In the *Toll2-2*^{RNAi} RLs, the relative amounts of *Toll* and *Toll6-2* mRNA were slightly reduced to 75% and 71%, respectively (Fig. S5B), but expression levels of other cricket Toll genes, including *Toll2-1*, were not significantly changed. These results suggest that the RNAi phenotypes observed in *Toll2-1*^{RNAi}

Development (2022) 149, dev199916. doi:10.1242/dev.199916

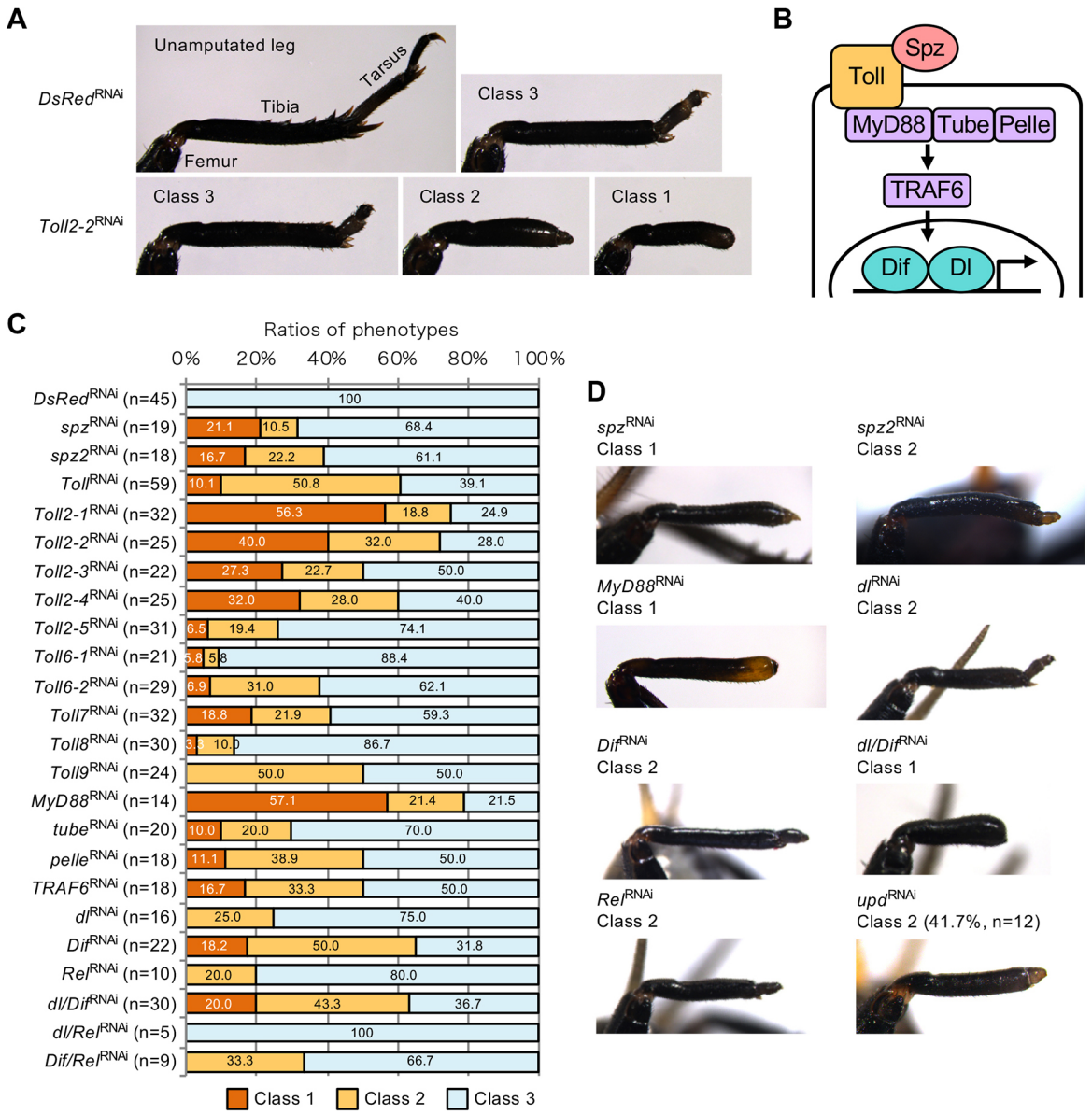

Fig. 3. Phenotypes after RNAi against Toll signalling component genes. (A) Typical morphology of an unamputated leg and RLs of *DsRed*^{RNAi} and *Toll2-2*^{RNAi} crickets at the fifth instar. Class 3 is a normal regeneration phenotype in which the lost parts of the tibia, tarsus and claw were successfully reconstructed. Class 1 is a defective regeneration phenotype in which the lost tarsus was not reconstructed. Class 2 is an impaired regeneration phenotype in which the lost tarsus and claw were regrown but were malformed. (B) Schematic of the molecules involved in Toll signalling. *Gryllus* genome has a single gene for each of *MyD88*, *tube*, *pelle* and *TRAF6* homologues, and there are two *spz* genes. (C) The percentage of RNAi phenotypes of class 1, class 2 and class 3. *n*=numbers of RNAi-treated individuals. (D) Typical morphology of RLs of frequently observed phenotypes for RNAi-treated crickets at fifth instar.

crickets might be caused by an additional reduction in the *Toll2-2* mRNA level. Nucleotide alignment indicated that an off-target effect was unlikely (Fig. S5C), implying a possible epistatic regulation of *Toll2-2* by *Toll2-1*.

We next focused on *Toll2-2* function during cricket leg regeneration by carrying out single-gene functional analysis by RNAi. Notably, 28% of *Toll2-2*^{RNAi} crickets exhibited a class 3 phenotype (Fig. 3C) and 36% of endogenous *Toll2-2* mRNA remained after *Toll2-2*^{RNAi} (Fig. S4A), implying that RNAi against *Toll2-2* could show dose dependency. We injected a larger volume of *Toll2-2* dsRNA solution (483 nl) and compared the resulting phenotypes with those obtained from standard *Toll2-2*^{RNAi} (207 nl). RNA reduction and phenotype ratio were not significantly different in either experimental condition (Fig. S6); therefore, for subsequent analyses, we performed RNAi using standard conditions.

Toll2-2 regulates blastema cell proliferation

To examine whether the class 1 or 2 phenotype observed in *Toll2-2*^{RNAi} crickets (Fig. 3A,C, Fig. 4) was caused by abnormal regulation of cell proliferation in the blastema, we analysed cell proliferation in *Toll2-2*^{RNAi} crickets at 48 hpa. The distribution of S-phase proliferating cell nuclei and total nuclei, revealed by 5-ethynyl-2-deoxyuridine (EdU) incorporation assay and Hoechst 33342 staining, respectively, was determined in *Toll2-2*^{RNAi} and *DsRed*^{RNAi} RLs (Fig. 5A). The proportions of S-phase nuclei out of all nuclei in the *Toll2-2*^{RNAi} and *DsRed*^{RNAi} RLs were 37.41±5.80% (*n*=4) and 3.63±2.26% (*n*=3), respectively (Fig. 5B).

Development (2022) 149, dev199916. doi:10.1242/dev.199916

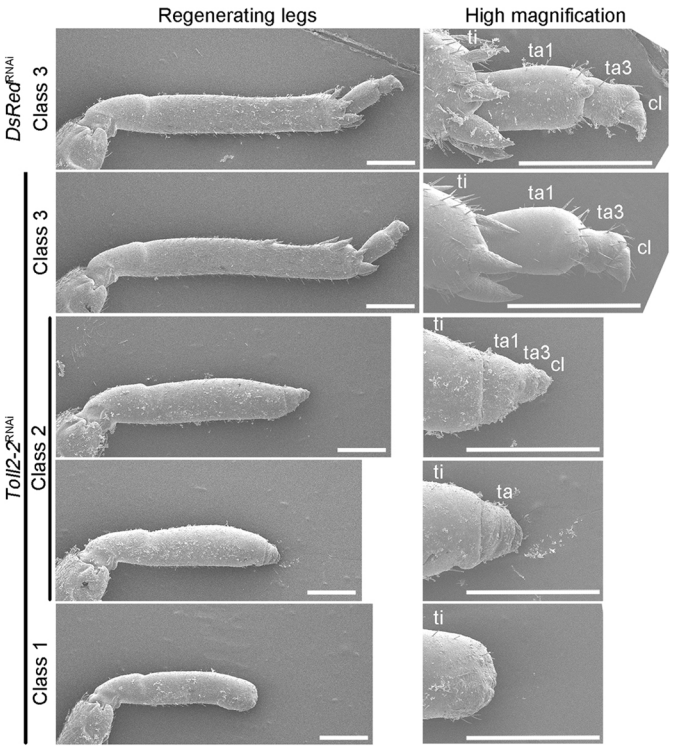

Fig. 4. Scanning electron microscopy of regenerating legs. Scanning electron microscopy images of *DsRed*^{RNAi} and *Toll2-2*^{RNAi} RLs at the fifth instar. Class 3 refers to normally regenerating legs of *DsRed*^{RNAi} and *Toll2-2*^{RNAi} crickets. Class 2 is an impaired regeneration phenotype in which the lost tarsus and claw were regrown but malformed. Class 1 is a defective regeneration phenotype in which the lost tarsus is not reconstructed. Right-hand panels show high-magnification images of the distal region of the tibiae and tarsi. cl, claw; ta, tarsal segment; ti, tibia. Scale bars: 500 µm.

M-phase proliferating cell nuclei were also revealed by anti-phosphorylated histone H3S10 antibody (PH3) staining (Fig. 5A). The proportions of the number of M-phase nuclei out of total nuclei in the control and *Toll2-2*^{RNAi} RLs were 4.05±1.53% (n=4) and 1.15±0.26% (n=3), respectively (Fig. 5B). The proportions of S- and M-phase cells were significantly decreased by *Toll2-2*^{RNAi} in the 48 hpa blastema. These histochemical observations were validated by qPCR of *Gryllus* cyclin genes. The relative amounts of *cycE* and *cycB* mRNA were significantly decreased to 49% and 47%, respectively, in *Toll2-2*^{RNAi} RLs compared with those of *DsRed*^{RNAi} (Fig. 5C).

Given that transcript levels of *Gryllus* cyclin genes are decreased in the regenerating leg after RNAi against JAK/STAT signalling component genes (Bando et al., 2013) (Fig. S1), we quantified the expression levels of the *Gryllus* homologues of JAK/STAT signalling component genes – *unpaired* (*upd*), *domeless* (*dome*), *hopscotch* (*hop*) and *Stat* in *Toll2-2*^{RNAi} RLs. Expression of *upd*, *dome* and *hop* was downregulated by *Toll2-2*^{RNAi} in RLs compared with those of *DsRed*^{RNAi} (Fig. 5D). To determine whether Toll2-2 signalling might regulate transcription of Toll ligand genes, we examined the expression of *spz* and *spz2* and found that it was decreased in *Toll2-2*^{RNAi} RLs (Fig. 5E). These results suggest that Toll2-2 signalling upregulates the expression of its own ligands, *spz/spz2*, as well as JAK/STAT signalling component genes and cyclins, or that Toll2-2 affects localisation of the ligand-expressing cells during *Gryllus* leg regeneration.

Plasmatocytes accumulate in the blastema region to promote leg regeneration

The results described above indicated that *Toll2-2* promotes cell proliferation during regeneration. In vertebrates, TLRs localise to the cell membrane of macrophages to detect infectious microbes (Satoh and Akira, 2016). In insects, including *G. bimaculatus*, plasmatocytes are professional phagocytic cells and are regarded as

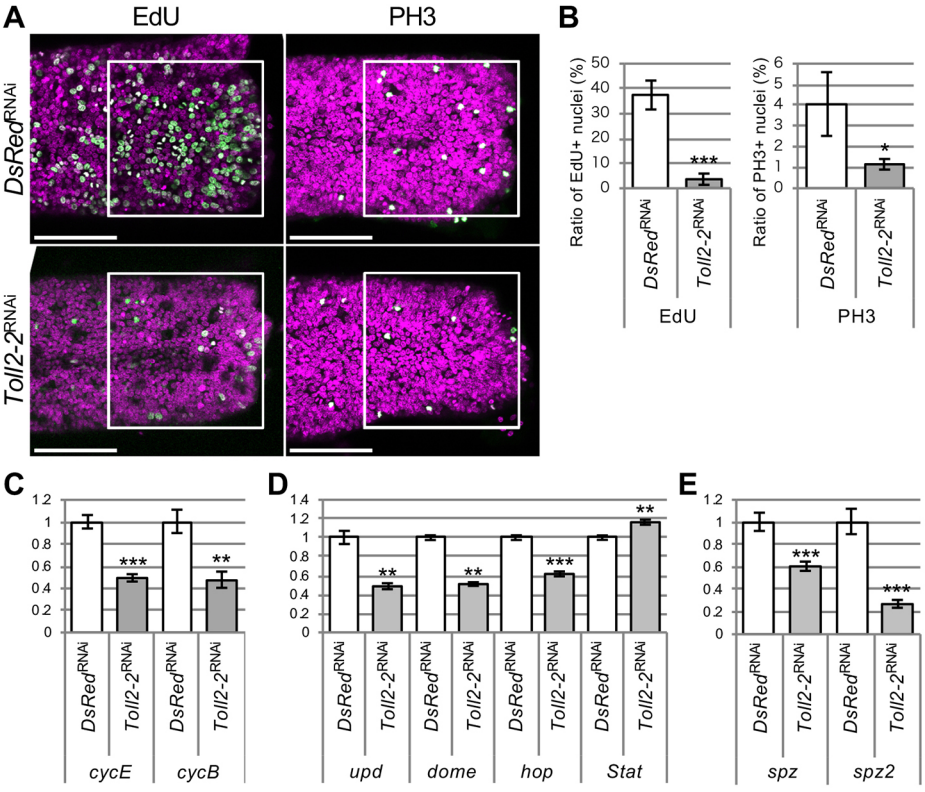

Fig. 5. Cell proliferation in *Toll2-2*^{RNAi} RLs. (A) Confocal images (*z*-stack) of the distribution of proliferating cells at the S phase and M phase by EdU-incorporation assay and anti-phosphorylated histone H3S10 (PH3) antibody staining in RLs of *DsRed*^{RNAi} and *Toll2-2*^{RNAi} crickets at 48 hpa. All nuclei are magenta, EdU-incorporated or PH3-positive nuclei are green. Scale bars: 100 µm. (B) Proportions of EdU-positive nuclei and PH3-positive nuclei compared with total nuclei indicated by Hoechst 33342 staining. The number of cells in the boxed area in A were counted. (C-E) Relative amounts of *cycE* and *cycB* (C), *upd*, *dome*, *hop* and *Stat* (D), and *spz* and *spz2* (E) transcripts in *DsRed*^{RNAi} and *Toll2-2*^{RNAi} RLs at 48 hpa. The *y*-axes indicate normalized expression after *DsRed*^{RNAi} and relative expression levels after *Toll2-2*^{RNAi}. **P*<0.05, ***P*<0.01, ****P*<0.001 (unpaired, two-tailed Student's *t*-test between *DsRed*^{RNAi} and *Toll2-2*^{RNAi} samples).

Development (2022) 149, dev199916. doi:10.1242/dev.199916

insect macrophages (Cho and Cho, 2019). To visualise the cricket presumptive plasmatocytes, India ink and boron-dipyrromethene-cholesterol within liposomes (BODIPY-lipo) were injected into the haemolymph of third instar nymph abdomens. India ink and BODIPY-lipo are characteristically incorporated into plasmatocytes. Thus, *Gryllus* plasmatocytes were identified by black droplets of India ink in Giemsa-stained smears and by green fluorescence of BODIPY-lipo (Fig. 6A). Phalloidin staining revealed the actin cytoskeleton of haemocytes and part of the haemocytes incorporated with BODIPY-lipo (Fig. 6B). During leg regeneration, plasmatocytes accumulated near the blastema region of the regenerating tibia, and some plasmatocytes remained in the femur (Fig. 6C). Accumulation of plasmatocytes into the blastema region was observed at 48 hpa compared with the pattern at 0 hpa (Fig. 6D), suggesting that plasmatocytes accumulate at the wound region following amputation.

To clarify the role of plasmatocytes in leg regeneration, plasmatocytes were depleted using 100 nm diameter Clo-lipo. The mean lifespan was estimated as the day when the survival rate was 50% after injection of Clo-lipo and PBS-lipo (liposome-encapsulated PBS buffer for control experiments). The mean lifespan of Clo-lipo-injected crickets was 15 days (Fig. S8A). To confirm the depletion of plasmatocytes, BODIPY-lipo was injected 24 h after the injection of Clo-lipo or PBS-lipo. The number of BODIPY-labelled plasmatocytes was decreased in the haemolymph of Clo-lipo-injected crickets compared with PBS-lipo-injected crickets (Fig. S8B). We also confirmed the depletion of plasmatocytes in the RLs at 48 hpa: Phalloidin-positive haemocytes were present beneath the epidermal cells in PBS-lipo- or Clo-lipo-injected RLs (Fig. 6E). However, BODIPY-incorporated plasmatocytes were not present in the blastema region of Clo-lipo-injected RLs (Fig. 6E).

To clarify the relationship between plasmatocyte function and leg regeneration, we observed the leg regeneration processes of Clo-lipo- and PBS-lipo-injected crickets. In PBS-lipo crickets, the wound surface was covered by a new cuticle at the fourth instar and

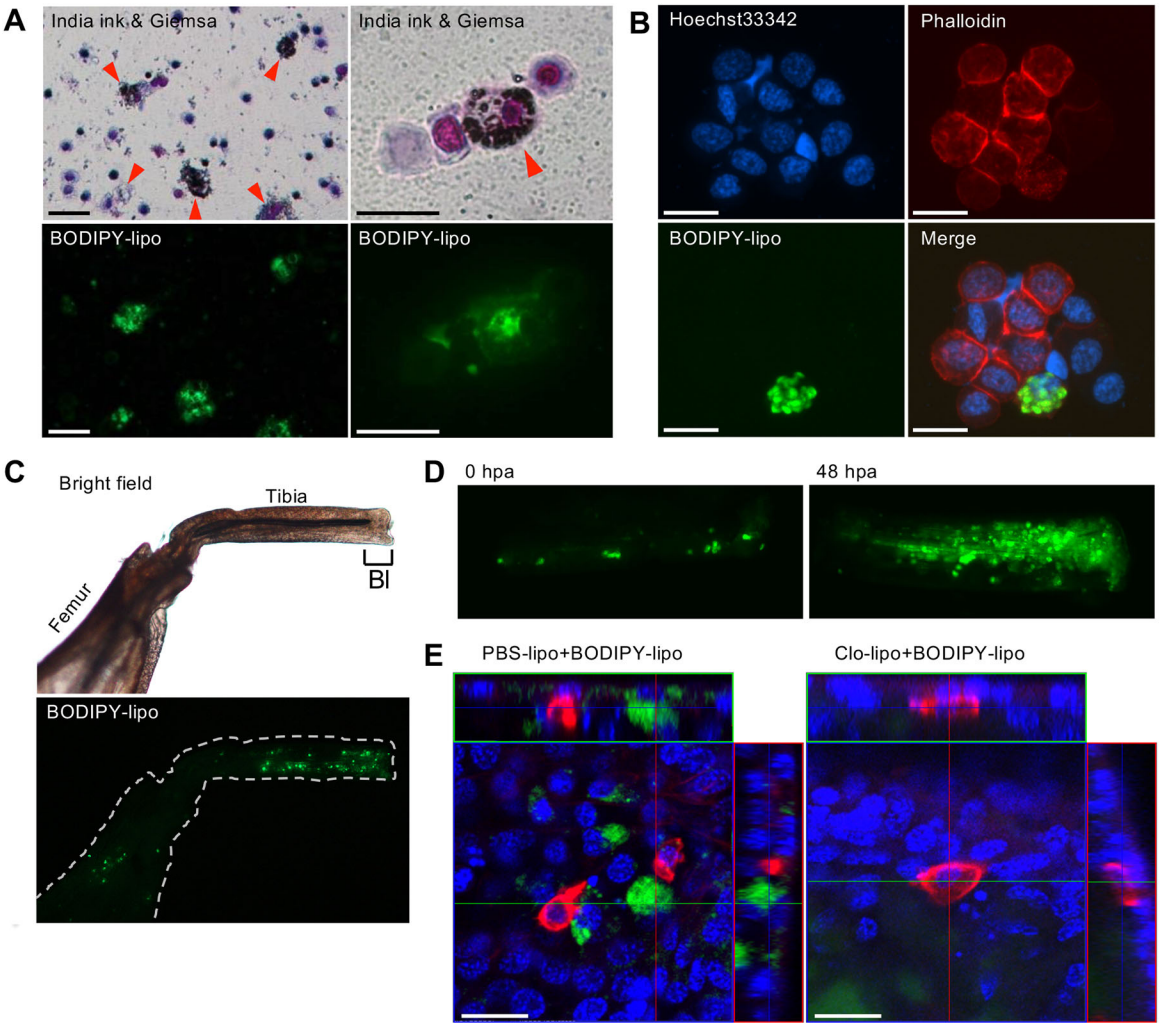

Fig. 6. Distribution of plasmatocytes in haemolymph and regenerating legs. (A) Smear samples of *Gryllus* haemolymphs were stained with Giemsa. Plasmatocytes (red arrowheads) are visualised by incorporation of India ink (top) and BODIPY-lipo (bottom). (B) Nuclei and actin cytoskeleton of haemocytes were stained by Hoechst 33342 and Rhodamine phalloidin, respectively. Plasmatocytes were visualised by BODIPY-lipo incorporation. (C) Distribution of plasmatocytes in a RL at 48 hpa was visualised by BODIPY-lipo incorporation. Blastema (Bl) is indicated by the bracket in the brightfield image. Dashed line marks the leg outline in the BODIPY-lipo image. (D) Distribution of plasmatocytes in RLs at 0 and 48 hpa were visualised by BODIPY-lipo incorporation. (E) Confocal images (*z*-stack) of the distribution of plasmatocytes in the blastema region of RLs of PBS-lipo-treated and Clo-lipo-treated crickets at 48 hpa. Plasmatocytes were visualised by BODIPY-lipo (green) and Rhodamine phalloidin (red), and nuclei were stained with Hoechst 33342 (blue). Cells with strong red fluorescence are likely spreading plasmatocytes with increased F-action expression (Williams, 2009; Xu et al., 2012). Scale bars: 20 µm.

Development (2022) 149, dev199916. doi:10.1242/dev.199916

the lost parts of the legs were regenerated by the sixth instar in a regeneration process that was indistinguishable from that of untreated crickets (Fig. 7A). In contrast, in Clo-lipo-injected crickets, the wound surface was covered by a new cuticle at the fourth instar, but the lost parts of the legs were not regenerated (class 1 phenotype) in 30/39 (76.9%) crickets or were regenerated in a small-malformed structure (class 2 phenotype) in 9/39 (23.1%) crickets (Fig. 7A). Reduction of plasmatocytes in the RLs at 48 hpa was quantified by qPCR for *Gryllus* homologues of *croquemort* (*crq*) and *glial cells missing* (*Gcm*), which are expressed in *Drosophila* plasmatocytes (Wang et al., 2014). A significant reduction in both gene expression was observed. Expression of *crq* was downregulated in Clo-lipo RLs compared with PBS-lipo RLs (P<0.001 by Student's t-test; Fig. 7B), indicating that Clo-lipo injection led to a decrease in the number of plasmatocytes in RLs .

The distribution of proliferating cells in the S and M phases was examined using the EdU-incorporation assay and anti-phosphorylated histone H3S10 antibody staining, respectively (Fig. 7D). In cricket RLs, the blastema appears as a whitish tissue localised in the distal region (Fig. 7C, brackets). In Clo-lipo RLs, however, scabs adhered to the wound surface. Thus, the wound epidermis and tibial epidermis were fragile when we removed the scab and cuticle from the RLs (Fig. 7C). The proportions of S- and M-phase cell nuclei out of total cell nuclei in the PBS-lipo- and Clo-lipo-injected RLs at 48 hpa were 27.57±7.83% (n=3) and 9.73±5.07% (n=3) for S phase, and 5.72±1.173% (n=3)

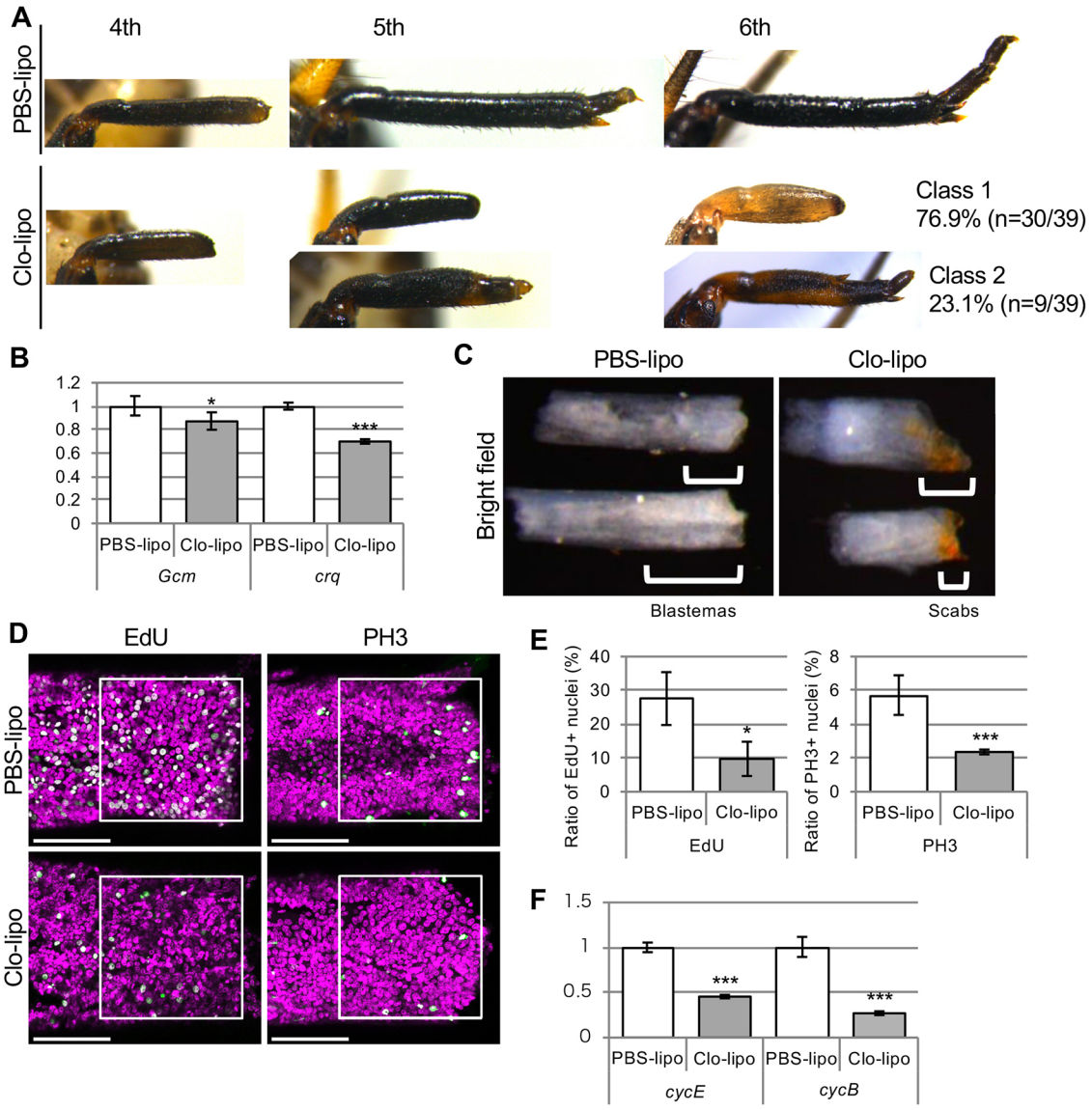

Fig. 7. Involvement of plasmatocytes in cricket leg regeneration. (A) Typical regeneration process of PBS-lipo- and Clo-lipo-incorporated crickets at fourth, fifth and sixth instar nymph stages. (B) Relative amounts of *Gcm* and *crq* transcripts in RLs of PBS-lipo- or Clo-lipo-incorporated crickets at 48 hpa. (C) Blastema formation in the PBS-lipo-incorporated RLs and scab formation in the Clo-lipo-incorporated RLs. Blastemas and scabs are indicated by brackets. (D) Confocal images (*z*-stack) showing proliferating cells at the S phase and M phase detected by EdU incorporation and anti-phosphorylated histone H3S10 (PH3) antibody staining, respectively, in PBS-lipo- or Clo-lipo-incorporated regenerating tibiae. Nuclei were stained with Hoechst 33342. All nuclei are magenta; EdU-incorporated or PH3-positive nuclei are green. Scale bars: 100 µm. (E) Proportions of EdU-positive nuclei and of PH3-positive nuclei compared with total nuclei. The number of cells in the boxed area in D was counted. (F) Relative amounts of *cycE* and *cycB* transcripts in RLs of PBS-lipo- or Clo-lipo-incorporated crickets. *P<0.05, ***P<0.001 (unpaired, two-tailed Student's t-test between PBS-lipo-incorporated and Clo-lipo-incorporated samples). In B,F, the y-axes indicate normalized expression of the PBS-lipo-treated samples and relative expression levels of Clo-lipo-treated samples.

Development (2022) 149, dev199916. doi:10.1242/dev.199916

and 2.35±0.14% (n=3) for M phase, respectively (Fig. 7E), a significant reduction in Clo-lipo RLs compared with PBS-lipo RLs (Fig. 7D,E). The relative amount of *cycE* and *cycB* transcripts was reduced to 45% and 27%, respectively, in Clo-lipo RLs compared with PBS-lipo RLs, as revealed by qPCR (Fig. 7F). The reduction of S- and M-phase cell nuclei and reduced expression of *cycE* and *cycB* observed in Clo-lipo-injected RLs (Fig. 7) were similar to those of the *Toll2-2*^{RNAi} RLs (Figs 3, 4 and 5).

Toll2-2 regulates accumulation of plasmatocytes into blastema

To clarify the link between plasmatocytes and Toll signalling, we sought to determine the Toll genes expressed in the plasmatocytes during leg regeneration. Haemolymph was collected from PBS-lipo-injected and Clo-lipo-injected regenerating cricket nymphs at 48 hpa. After RNA extraction and reverse transcription, the expression levels of Toll genes in the haemolymph samples were compared by qPCR. Because the number of plasmatocytes was lower in Clo-lipo-injected haemolymphs (Fig. S8B), transcripts expressed in other haemocytes might be relatively increased in mRNA from Clo-lipo-injected crickets compared with that of PBS-lipo-injected crickets. mRNA expression levels of *Toll2-1*, *Toll2-2* and *Toll2-5* were significantly decreased in Clo-lipo-injected haemolymph (Fig. 8A), suggesting that *Toll2-1*, *Toll2-2* and *Toll2-5* are dominantly expressed in plasmatocytes. In contrast, expression levels of *Toll2-4* and *Toll6-1* were significantly increased and that of *Toll2-3* was slightly increased in Clo-lipo-injected haemolymph (Fig. 8A), suggesting that *Toll2-4* and *Toll6-1* genes might be expressed in other types of haemocytes in addition to phagocytic plasmatocytes.

Next, the distribution of plasmatocytes in the *Toll2-2*^{RNAi} RLs was visualised and compared with those in *DsRed*^{RNAi}, PBS-lipo-injected, and Clo-lipo-injected RLs. BODIPY-lipo-incorporating plasmatocytes accumulated in the blastemas in the *DsRed*^{RNAi} and PBS-lipo-injected RLs (Fig. 8B, left). In contrast, few plasmatocytes accumulated in the Clo-lipo-injected blastema (Fig. 8B, bottom right), similar to what was seen in the Clo-lipo-injected haemolymphs (Fig. S8B). The number of BODIPY-lipo-incorporated plasmatocytes was decreased in *Toll2-2*^{RNAi} blastemas compared with *DsRed*^{RNAi} blastema (Fig. 8B, top). The BODIPY-lipo-incorporated plasmatocytes in the blastema were counted and the number of cells in the same volume of blastemas was calculated for comparison. In *DsRed*^{RNAi} and PBS-lipo-incorporated RLs, 16.6±3.5 (n=4) and 18.6±3.7 (n=7) plasmatocytes, respectively, accumulated in the blastema in a volume of 2.5×10^5 µm^3 . In contrast, accumulated plasmatocytes were significantly decreased to 10.7±2.1 and 3.4±2.3 in the *Toll2-2*^{RNAi} (n=4) and Clo-lipo-incorporated (n=6) RLs, respectively, in the same volume (Fig. 8C), indicating that *Toll2-2*^{RNAi} reduced the accumulation of plasmatocytes into the blastemas.

In vertebrates, activated macrophages release cytokines to stimulate other immune cells. In *Drosophila*, haemocytes release

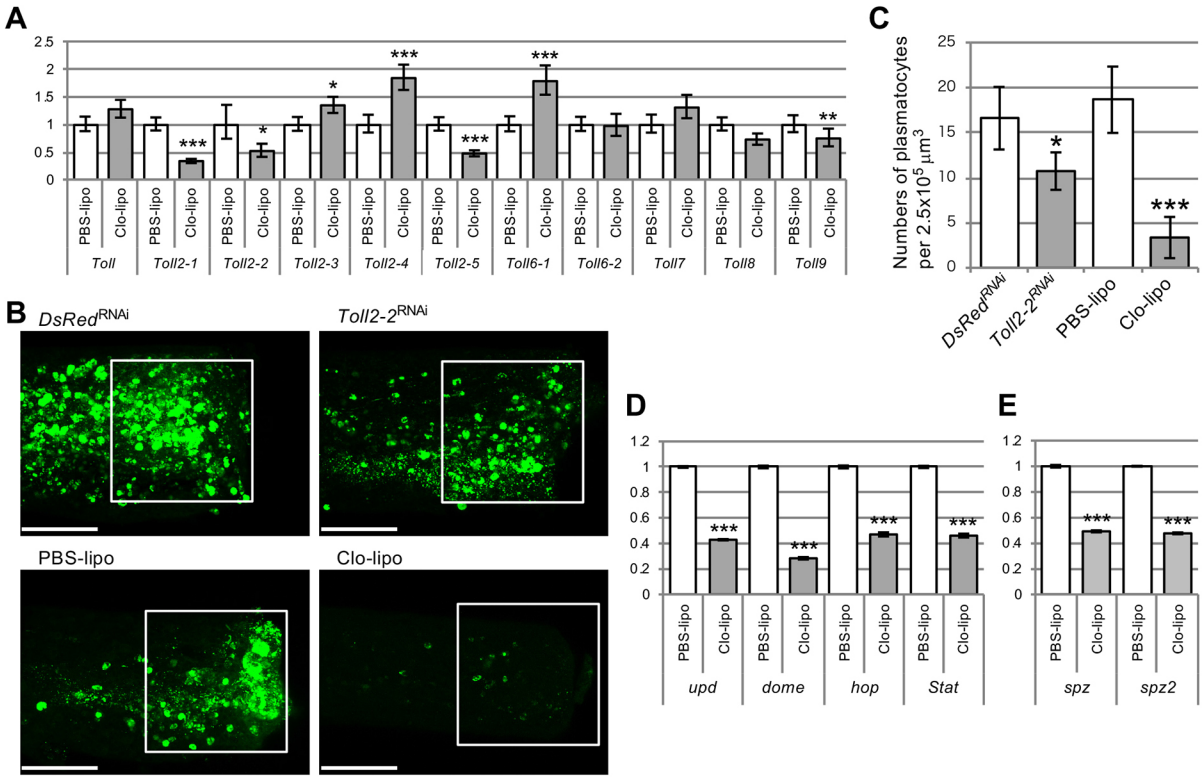

Fig. 8. Involvement of *Toll2-2* in plasmatocyte accumulation during leg regeneration. (A) Relative amounts of transcripts of *Gryllus* Toll genes in PBS-lipo-treated haemolymph and Clo-lipo-treated haemolymph. **P*<0.05, ***P*<0.01, ****P*<0.001 (unpaired, two-tailed Student's *t*-test between PBS-lipo-incorporated and Clo-lipo-incorporated samples). (B) Confocal images (*z*-stack) showing the distribution of plasmatocytes, indicated by BODIPY-lipo incorporation, in RLs at 48 hpa of *DsRed*^{RNAi}, *Toll2-2*^{RNAi}, PBS-lipo-incorporated and Clo-lipo-incorporated blastemas. Scale bars: 100 µm. (C) Numbers of BODIPY-lipo-incorporating plasmatocytes per volume in RLs. **P*<0.05, ****P*<0.001 (unpaired, two-tailed Student's *t*-test between *DsRed*^{RNAi} and *Toll2-2*^{RNAi} samples, and between PBS-lipo-incorporated and Clo-lipo-incorporated samples). (D,E) Relative amounts of transcripts of JAK/STAT signalling component genes (D) and *spz* and *spz2* (E) in RLs of PBS-lipo- or Clo-lipo-incorporated crickets at 48 hpa. ****P*<0.001 (unpaired, two-tailed Student's *t*-test). In A,D,E, the *y*-axes indicate normalized expression of the PBS-lipo-treated samples and relative expression levels of Clo-lipo-treated samples.

Development (2022) 149, dev199916. doi:10.1242/dev.199916

insect cytokines, including Upd and Spz, to induce an immune response (Agaisse et al., 2003; Shaukat et al., 2015). In Clo-lipo RLs, the relative expression levels of *upd*, *spz* and *spz2* were significantly decreased to 43%, 49% and 48%, respectively, compared with PBS-lipo RLs (Fig. 8D,E). Taken together with the downregulation of *upd*, *spz* and *spz2* in *Toll2-2*^{RNAi} RLs (Fig. 5D,E) and defective regeneration phenotypes caused by RNAi of each of these genes (Fig. 3C,D), the collective data suggest that Upd and Spz/Spz2 activate the JAK/STAT and Toll signalling pathways, respectively, during *Gryllus* leg regeneration. Thus, plasmatocytes that accumulate in RLs release cytokines, which activate the JAK/STAT and Toll signalling pathways, leading to blastemal cell proliferation during cricket leg regeneration.

Infectious microbes do not have a major role in leg regeneration

In mammals, PAMPs, including lipopolysaccharides, lipoproteins and flagellin, directly bind to TLRs (Pandey et al., 2014). In insects, PGRPs detect PAMPs, leading to the activation of Toll or Imd signalling pathways to produce antimicrobial peptides (AMPs) (Lemaitre and Hoffmann, 2007; Lemaitre et al., 1996; Lindsay and Wasserman, 2014) (Fig. S1). To identify whether pathogen infection is a trigger for regeneration, we cloned partial cDNA fragments of *Gryllus* homologous genes of *PGRP-SA* and *PGRP-SD*, which recognise gram-positive bacteria, and *PGRP-LC* and *imd*, which recognise gram-negative bacteria, and performed RNAi to observe phenotypes of regenerating legs. The *Gryllus* genome encodes a single gene for each of the four genes. Determination of leg regeneration phenotypes after *PGRP-SA*^{RNAi}, *PGRP-SD*^{RNAi}, *PGRP-LC*^{RNAi} and *imd*^{RNAi} revealed that all crickets regenerated legs normally, in a similar manner to *DsRed*^{RNAi} crickets (Fig. S9A). This finding indicates that infectious microbes do not play a major role in leg regeneration. To further substantiate this, we examined the gene expression change of the *Gryllus* homologue of *defensin*, which encodes an evolutionarily conserved AMP (Fig. S10). qPCR analysis revealed that the expression level of *Gryllus defensin* was decreased at 3, 24 and 48 hpa in RLs (Fig. S10C), suggesting that PAMP-mediated activation of Toll signalling is suppressed during regeneration.

Toll molecules recognise PAMPs and DAMPs, mediated by clip-SP Persephone in *Drosophila* (Ming et al., 2014). We could not find a *persephone* (*psh*) homologue in the *Gryllus* genome (Fig. S11). DAMPs are released from cells in response to injury or cell death, including apoptosis and necrosis. We focused on the function of the scavenger receptor CD36 homologue Crq, which recognises the apoptotic body and is required for phagocytosis of plasmatocytes in *Drosophila*. The *Gryllus crq* homologue was expressed in plasmatocytes (Fig. 7B). During leg regeneration, 16.7% and 45.8% of *crq*^{RNAi} crickets had class 1 and class 2 phenotype, respectively (Fig. S9B-D). These results suggest that recognition and engulfment of apoptotic bodies released from injured cells by Crq likely triggers leg regeneration in crickets.

DISCUSSION

Toll-related signalling, rather than Imd signalling, is a major pathway in cricket leg regeneration from the early phases

Toll/TLR signalling is evolutionarily conserved from insects to humans for the recognition of pathogens including viruses, gram-positive bacteria and fungi (Lindsay and Wasserman, 2014; Pandey et al., 2014). Toll/TLRs induce gene expression of cytokines and antibacterial components via MyD88 and NF-κB (Lemaitre and Hoffmann, 2007), although *Drosophila* Toll-2 does not require MyD88 for cell proliferation (Li et al., 2020). In insect immunity, activation of Toll signalling is different from that of vertebrates; infectious microbes are detected by PGRPs that activate clip-SPs to catalyse pro-Spz to Spz, which binds to a Toll receptor to activate signalling (Fig. S1) (Krautz et al., 2014; Lindsay and Wasserman, 2014). We previously reported that expression of *Spz*, Toll receptors and NF-κB (*Relish*, *dl*) genes is upregulated in RLs at 24 hpa (Bando et al., 2013). In this study, RNA-seq data showed that the expression of three *Gryllus* Toll genes (*Toll2-2*, *Toll2-5*, *Toll8*) and *Rel* were upregulated as early as at 3 hpa in RLs. Upregulation of *Toll2-1*, *Toll2-2* and *Toll2-5* genes was confirmed by qPCR during regeneration, suggesting that Toll signalling is involved in the cricket regeneration process from the early phases.

Imd signalling, another pathway involved in insect immunity (Fig. S1), detects infections by gram-negative bacteria. PGRP-LC and Imd together induce the expression of antibacterial components through the NF-κB transcription factor Rel (Krautz et al., 2014; Lemaitre and Hoffmann, 2007). Although expression of *Rel* was upregulated in 3 hpa RLs (Fig. S2B), RNAi of *PGRP-LC*, *imd* and *Rel* did not show obvious defects in leg regeneration (Fig. 3C,D, Fig. S9A), suggesting that Imd signalling is not essential for leg regeneration in *G. bimaculatus*.

Our previous study showed that JAK/STAT signalling is involved in leg regeneration (Bando et al., 2013). Ligands for JAK/STAT signalling are interleukins in vertebrates (Morris et al., 2018). In *Xenopus* tadpole tail regeneration, interleukin-11 induces undifferentiation state (Tsujioka et al., 2017). In *Drosophila melanogaster*, ligands of JAK/STAT signalling are Upds, which act as cytokines (Arbouzova and Zeidler, 2006) and are required for the regulation of stem cell proliferation during intestinal regeneration (Kux and Pitsouli, 2014). In the present study, the expression of *upd* was decreased in plasmatocyte-depleted RLs. Lost parts of legs of *upd*^{RNAi} crickets were not fully regenerated, similar to observations after RNAi of JAK/STAT signalling genes (Bando et al., 2013). In a similar manner to the production of interleukins by macrophages to activate other immune cells in vertebrates (Schett et al., 2016), plasmatocytes release insect cytokines to induce the production of antibacterial components in *Drosophila* (Lemaitre and Hoffmann, 2007; Ramond et al., 2020). Thus, it is likely that *Gryllus* plasmatocytes produce Upd to activate JAK/STAT signalling in leg regeneration.

Toll-related signalling promotes leg regeneration by controlling cell proliferation during blastema formation

We cloned 11 Toll genes from *Gryllus*, not all of which were directly homologous to those of the nine Toll genes of *Drosophila* (Hillyer, 2016). The *Gryllus* genome has five *Toll2* paralogues (*Toll2-1–5*) that are not present in *Drosophila*, and two *Toll6* paralogues (*Toll6-1–2*). *Gryllus* has no genes homologous to *Drosophila Toll3*, *Toll4* and *Toll5*. *Drosophila* Toll (McIlroy et al., 2013; McLaughlin et al., 2016; Ward et al., 2015) is important for defence against pathogens (Lemaitre and Hoffmann, 2007) and dorsoventral patterning during embryogenesis (Moussian and Roth, 2005). Toll-2, -6 and -8 are involved in the anteroposterior patterning of the fly (Paré et al., 2014). *Drosophila* Toll-2 regulates cell proliferation and planar cell polarity (Li et al., 2020; Tamada et al., 2021) and Toll-6 promotes neuronal cell shape, survival and interactions (McIlroy et al., 2013; McLaughlin et al., 2016; Ward et al., 2015). In *Gryllus*, *Toll6-1*, *Toll6-2*, *Toll7* and *Toll8* are expressed during embryogenesis (Benton et al., 2016). Their functions related to immunity and dorsoventral patterning are unknown. This study has clarified that diversified *Gryllus* Toll2

Development (2022) 149, dev199916. doi:10.1242/dev.199916

subfamily members play crucial roles in the early phase of leg regeneration.

Expression of *Toll2-1*, *Toll2-2* and *Toll2-5* was upregulated during leg regeneration, in which >70% of *Toll2-2*^{RNAi} crickets showed regeneration defects. The proportions of S- and M-phase proliferating cells were decreased in *Toll2-2*^{RNAi} RLs, indicating that Toll2-2 signalling is required for cell proliferation during leg regeneration. In *Toll2-2*^{RNAi} RLs, accumulation of plasmatocytes was reduced and expression of *upd* was downregulated. Thus, *Toll2-2* in plasmatocytes may induce *upd* expression, which activates the JAK/STAT signalling pathway (Bando et al., 2013) and cyclins, leading to cell proliferation in regenerating legs.

During early leg regeneration processes, expression of *Toll2-4*, *Toll6-1*, *Toll6-2*, *Toll7*, *Toll8* and *Toll9* was decreased (Fig. 2B). However, *Toll2-4*^{RNAi}, *Toll6-2*^{RNAi}, *Toll7*^{RNAi} and *Toll9*^{RNAi} crickets showed defective or impaired regeneration phenotypes (Fig. 3C). *Toll2-4*^{RNAi}, *Toll6-2*^{RNAi}, *Toll7*^{RNAi} and *Toll9*^{RNAi} decreased target gene transcripts by >40%, verifying the RNAi efficiency (Fig. S4A). Our preliminary study showed that RNAi of cricket nymphs continued to suppress target gene expression for 2 weeks. Therefore, it is possible that the continuous suppression of gene expression caused defective or impaired regeneration phenotypes in *Toll2-4*^{RNAi}, *Toll6-2*^{RNAi}, *Toll7*^{RNAi} and *Toll9*^{RNAi} crickets.

Crosstalk between Toll signalling and Hippo signalling, and between Hippo signalling and JAK/STAT signalling may also regulate tissue growth (Liu et al., 2016; Jiang et al., 2016). Specifically, the Hippo signalling component Warts, together with protocadherins Fat and Dachsous, suppresses blastema cell proliferation, whereas Yorkie promotes proliferation during cricket leg regeneration (Bando et al., 2009). Therefore, Toll signalling may interfere with Hippo signalling to regulate blastema cell proliferation in crickets, although *Drosophila* Toll-2 cooperatively promotes cell proliferation with Yki (Li et al., 2020).

Plasmatocytes (insect macrophages) promote leg regeneration in the cricket, via Spz-Toll-related and Upd-JAK/STAT signalling

Insect haemocytes play a major role in host defence (Lavine and Strand, 2002; Ribeiro and Brehélin, 2006), as insects have an open blood-vascular system and lack oxygen-carrying erythrocytes. Insect haemocytes vary depending on the species. For example, the cricket *G. bimaculatus* has plasmatocytes, granulocytes, and three or four other haemocytes (Cho and Cho, 2019; Sokolova et al., 2000). Plasmatocytes in several insect species engulf pathogens and produce inflammatory cytokines and antipathogenic components (Evans et al., 2003; Lavine and Strand, 2002). In the present study, plasmatocyte-depleted crickets did not regenerate missing leg parts. Given that cytokines promote regeneration in axolotl and zebrafish (Godwin et al., 2013; Petrie et al., 2014), cricket plasmatocytes could promote tissue regeneration, possibly by these evolutionarily conserved molecular mechanisms. Although we had no direct evidence for localisation of the *Toll2-1*, *Toll2-2* and *Toll2-5* genes in plasmatocytes, their reduced expression levels in plasmatocyte-depleted haemocytes strongly support this idea. Likewise, the finding that cricket plasmatocytes express the cytokine genes *upd*, *spz* and *spz2* is reminiscent of the secretion of interleukins from axolotl macrophages during regeneration (Godwin et al., 2013).

Toll-related signalling senses cell debris caused by injury and promotes regeneration

Mammalian TLRs are pattern recognition receptors, but *Drosophila* Tolls are not, as they bind endogenous ligands instead of pathogens (Krautz et al., 2014; Lindsay and Wasserman, 2014; Pandey et al., 2014). When pathogens are recognised by PGRPs, the PGRPs catalyse the maturation of pro-Spz to Spz. Spz subsequently binds to Toll proteins to activate Toll signalling. In the present study, crickets subjected to RNAi of the pathogen recognition protein-coding genes *PGRP-SA*, *PGRP-SD*, *PGRP-LC* or *imd* showed normal regeneration (Fig. S9A). Expression of the antimicrobial peptide gene *defensin* was not upregulated during regeneration (Fig. S10C), although the upstream region of the *defensin* gene contains many NF-κB-binding sites (Fig. S10D). This suggests that pathogen infection is not required for leg regeneration. Thus, non-pathogenic molecules may activate *Gryllus* Toll signalling during leg regeneration. Candidate molecules include DAMPs (Krautz et al., 2014), which are endogenous proteins that are likely released from injured cells, such as necrotic or apoptotic cells, and are recognised by specific receptors, such as RAGE, TREM1 and TLRs, in vertebrates (Piccinini and Midwood, 2010; Wang et al., 2015). The evolutionarily conserved proteins HMGB1, S100, HSP, histone, actin, DNA and RNA are well-known DAMPs (Piccinini and Midwood, 2010). In the mammalian kidney, DAMPs released from dying cells cause inflammatory responses and acute injury. Regeneration is accelerated by the TLR-mediated release of interleukins from macrophages or dendritic cells (Kulkarni et al., 2014). In the liver, denatured DNA from dying hepatocytes stimulates TLRs to mediate hepatocyte stem cell differentiation (Seki et al., 2011). RAGE and TREM1 are not conserved among insects; hence, Toll signalling is able to respond to DAMPs in insects. In *Drosophila*, the clip-SP Psh is involved in DAMP recognition and catalyses Pro-Spz to Spz to activate Tolls (Ming et al., 2014). The *psh* homologue is not present in the *Gryllus* genome (Ylla et al., 2021), but a *snake* homologue and three *grass* paralogues, which encode other clip-SPs, are (Fig. S11). Some of these genes may replace a particular role of *psh*.

Crq, which is a scavenger receptor CD36 homologue, is expressed in the plasmatocytes and is required for engulfment of apoptotic cells in *Drosophila* (Franc et al., 1996, 1999; Guillou et al., 2016). In mice, CD36 mediates phagocytosis by cooperating with TLR (Erdman et al., 2009). In the present study, *crq*^{RNAi} crickets showed defective and impaired regeneration phenotypes, similar to those found in *Toll2-2*^{RNAi} crickets. As mentioned above, RNAi of PGRP genes and *imd* resulted in normal regeneration, implying that the defective and impaired regeneration phenotypes caused by *crq*^{RNAi} and *Toll2-2*^{RNAi} could occur as a result of defects in phagocytosis of cell debris after injury. We propose that Toll2-2 and Crq cooperatively recognise damage-associated molecules near the wound region (Fig. S12).

Our cricket leg amputation experiments were conducted without artificial pathogen inoculation. In the early phase of leg regeneration, when blastema cells form, activated plasmatocytes migrate to the injury site and facilitate the proliferation of blastema cells. These plasmatocytes are most likely polarised toward enhanced phagocytic function by regulating Toll-related and JAK/STAT signalling (Fig. S1). The extent of plasmatocyte polarisation would be influenced by surrounding tissue damage and pathogenic status. Recent single-cell studies of plasmatocytes (Cattenoz et al., 2020) suggest that *crq*-expressing cells and *Toll-2-2*-expressing cells would not be identical subpopulations in the plasmatocytes during early cricket leg regeneration, which will require further study.

In conclusion, this study provides new insights into the function of Toll-related signalling for leg regeneration via plasmatocytes, cooperatively with JAK/STAT signalling. Recognition of apoptotic

Development (2022) 149, dev199916. doi:10.1242/dev.199916

cells via the scavenger receptor Crq on plasmatocytes also promotes leg regeneration.

MATERIALS AND METHODS

Animals

All nymphal and adult two-spotted crickets (*G. bimaculatus*) were reared under standard conditions (Mito and Noji, 2008). Third instar nymphs were used for RNAi and liposome injection to analyse the regeneration processes (Nakamura et al., 2008a).

RNA-seq

The distal one-third tibial regions of regenerating legs at 0 hpa (NLs) and 3 hpa (RLs) were separately collected from a few hundred crickets. Total RNA was extracted using ISOGEN II (311-07361, Nippon Gene). Poly(A)+ RNAs were purified using a MicroPoly(A)Purist kit (AM1919, Thermo Fisher Scientific). The cDNA libraries constructed from poly(A)+ RNAs were sequenced using a GS FLX Titanium next-generation sequencer (454 Life Sciences). To construct the assembled transcripts, the 595,425 reads of NL and 519,961 reads of RL samples (14,368,694 bp in total) that were sequenced were assembled into 20,317 contigs using GS De Novo Assembler v2.8 software. The average length of the assembled contigs was 2252 bp. To estimate the normalized expression levels of each transcript, each read obtained from the RL and NL samples was mapped to the contigs to calculate the RPKM value using GS Reference Mapper v2.8 software. Expression changes of assembled transcripts were calculated by dividing the RPKM values of RLs by corresponding RPKM value of NLs, which are listed in Table S1. Assembled transcripts that were upregulated more than twofold in RLs compared with NLs were annotated with the BLASTX program against the NCBI non-redundant protein sequence database, with an E-value cut-off of 0.001 (Table S2). Functional annotation of BLASTed transcripts was performed using Blast2GO software (https://www.blast2go.com/).

Cloning for *Gryllus* homologous genes

Gryllus homologues were cloned by PCR with Ex-taq or LA-taq with GC buffer (RR006A or RR02AG, TaKaRa Bio). Primers used are listed in Table S3. Template cDNAs were reverse transcribed using the SuperScript III reverse transcription kit with random primers (18080051, Thermo Fisher Scientific) from total RNA extracted from the regenerating legs of cricket nymphs at the third instar. The isolated *Gryllus* cDNA fragments were used as templates for the synthesis of dsRNAs.

RNAi

dsRNAs were synthesised using the MEGAScript T7 Kit (AMB13345, Thermo Fisher Scientific) and adjusted to 20 µM. Third instar nymphs were anaesthetised on ice before RNAi. After injection of 207 nl of dsRNA into the abdomen of the third instar nymphs with an auto-nanoliter injector (Nanoject II, #3-000-204, Drummond Scientific Company), their tibiae were amputated between the second and third spines. Wound regions are usually covered with scab within a day in third instar. The third instar nymphs moult to fourth instar within 4 days. In the fourth instar, newly formed cuticles cover the wound region instead of the scab. The fourth instar nymphs moult to fifth instar within 5 days and the lost leg tissues are reconstructed in miniature in the fifth instar. After RNAi and leg amputation, we observed RNAi phenotypes of regenerating legs on the 10th day, which corresponds to the late fifth instar. As a negative control for RNAi experiments, we injected dsRNA for the *DsRed2* exogenous gene. For dual RNAi experiments, a mixture of dsRNAs for the two target genes was used. In the mixture, the final concentration of each dsRNA was adjusted to 10 µM. Statistical differences in RNAi phenotypes were analysed by Fisher's exact test. For RNAi against *Toll* and *Toll2-2*, we generated two non-overlapping dsRNAs corresponding to either the 5′ or 3′ portion of the coding region (Fig. S3B, denoted by double-headed arrows). The RNAi experiments performed with these sequences were designated *Toll(5′)*^{RNAi}, *Toll(3′)*^{RNAi}, *Toll2-2(5′)*^{RNAi} and *Toll2-2(3′)*^{RNAi}, respectively.

qPCR

Regenerating tibiae of control, RNAi-treated or liposome-injected nymphs were pooled into single tubes, and total RNA was extracted using the RNAqueous-Micro Kit (AM1931, Thermo Fisher Scientific). Each pooled RNA sample was divided into two samples and reverse transcribed to prepare cDNA. Each cDNA was used for qPCR performed with the FastStart Essential DNA Green Master kit (06402712001, Roche) and the LightCycler Nano System (Roche). The relative proportions of the transcripts were calculated using *Gryllus* β-actin as an internal control. Relative gene expression levels are shown as the mean±s.d. Statistical differences were analysed by an unpaired, two-tailed Student's *t*-test between two samples or Tukey's test for more than three samples and are shown by asterisks (*P<0.05, **P<0.01, ***P<0.001). The qPCR experiments were repeated twice for confirmation. The primers used are listed in Table S4.

Cell proliferation assay

Proliferating cells in the S phase were detected using the Click-iT EdU Alexa Fluor 488 Imaging Kit (C10337, Thermo Fisher Scientific). EdU was injected into the abdomen of third instar cricket nymphs at 44 hpa, and the RLs were fixed at 48 hpa (4 h after EdU injection) with 2% paraformaldehyde (PFA) in PBS containing 0.05% Tween-20 (PBT) overnight at 4°C. EdU-incorporated cells were detected according to the manufacturer's instructions. Hoechst 33342 (H3570, Thermo Fisher Scientific) was used for nuclear staining. Proliferating cells in the M phase were detected by immunostaining of phospho-histone H3S10. Regenerating legs at 48 hpa were fixed with 2% PFA and cuticles were removed, then regenerating tibiae were washed with PBT and blocked with 1% normal goat serum (NGS) in PBT for 1 h. Blocked samples were incubated with primary antibody [rabbit polyclonal anti-phospho-histone H3 (Ser10) antibody; 06-570, Millipore] at 1:500 in 1% NGS in PBT overnight at 4°C. The samples were washed with PBT and blocked with 1% NGS in PBT. The samples were incubated with secondary antibody (Alexa Fluor 488-conjugated anti-rabbit IgG antibody; A-11008, Molecular Probes) at 1:750 in 1% NGS in PBT for 3 h at 25°C. Finally, the samples were washed with PBT and incubated with a 1:1000 dilution of Hoechst 33342 in PBT for 15 min.

Macrophage depletion and detection

For plasmatocyte depletion in crickets, 207 nl of Clo-lipo 100 (6.4 mg/ml clodronate) and Clo-lipo 300 (9.8 mg/ml clodronate) (160-0432-1 and 160-0430-1, Katayama Chemical Industries) was injected into the abdomen of third instar nymphs. PBS-encapsulated liposomes were used as controls. For plasmatocyte detection in the haemolymph, 207 nl India ink or 207 nl BODIPY-lipo (130 µg/ml BODIPY-cholesterol, Katayama Chemical Industries) were injected into the abdomen of third instar nymphs. One day after the injection, an anticoagulant solution (20 mM EDTA in PBS) was injected into the abdomen of the nymphs and haemolymphs were sucked from the nymphs. Haemolymphs were fixed with 2% PFA in an anticoagulant solution for 30 min at 25°C. Fixed haemocytes were washed with anticoagulant solution and then stained with a 1:2000 dilution of Hoechst 33342 for 30 min at 25°C. The haemocytes were washed with an anticoagulant solution and stained with a 1:40 dilution of Rhodamine phalloidin (R415, Thermo Fisher Scientific) for 30 min at 25°C. For plasmatocyte detection in the RLs, RLs of BODIPY-lipo-injected crickets at 48 hpa were fixed with 2% PFA in PBT and the cuticles were removed. Stained haemocytes and cuticle-removed RLs were observed with a fluorescent microscope DM5000 B (Leica Microsystems), and with a confocal laser scanning microscope LSM780 (Carl Zeiss) at the Central Research Laboratory, Okayama University Medical School, Okayama, Japan.

Scanning electron microscopy

Scanning electron microscopy images of RLs at the fifth instar were obtained. RLs of control and *Toll2-2*^{RNAi} were fixed in 4% PFA and 4% glutaraldehyde in PBS for 15 min at room temperature. Fixed legs were washed with PBS, then dehydrated through an alcohol series (20%, 40% and 60% ethanol in PBS, 80% ethanol in water, 45% ethanol and 45% tert-butyl alcohol in water) for 30 min and in 100% tert-butyl alcohol for 1 h. After dehydration, the fixed legs were substituted with 100% tert-butyl alcohol, frozen at 4°C, and freeze-dried. Dried legs were coated with osmium with

osmium coater (HPC-1S; VACUUM DEVICE). Images were captured using a model S-4800 field emission scanning electron microscope (Hitachi) at the Central Research Laboratory, Okayama University Medical School, Okayama, Japan.

Acknowledgements
We are grateful to Dr Itsuro Sugimura (Hokkaido System Science Co., Ltd.) for assistance with data analysis; Dr Takayuki Otani (Katayama Chemical Industries Co., Ltd.) for preparing PBS-lipo, Clo-lipo and BODIPY-lipo; and Nobuaki Fujimori and Taiki Morino for their technical assistance.

Competing interests
The authors declare no competing or financial interests.

Author contributions
Conceptualization: T.B., M.O., K.A., S.N., H.O.; Methodology: T.B., M.O., Y.I., E.K., T.I., K.A., S.N.; Validation: T.B., M.O., Y.B., M.H., Y.H., E.K., T.I.; Formal analysis: T.B., M.O., Y.B., M.H., Y.H., E.K., T.I.; Investigation: T.B., M.O., Y.B., M.H., Y.H., Y.I., E.K., T.I.; Resources: T.B., M.O., Y.B., M.H., Y.H., E.K., T.I., S.N.; Data curation: T.B., M.O., Y.B., M.H., Y.H., Y.I., E.K., T.I., H.O.; Writing - original draft: T.B., M.O.; Writing - review & editing: T.B., Y.H., T.M., K.A., S.N., H.O.; Visualization: T.B., M.O., Y.B., M.H.; Supervision: T.B., K.A., S.N., H.O.; Project administration: T.B., S.N., H.O.; Funding acquisition: T.B., T.M., K.A., S.N., H.O.

Funding
This work was supported by a Grant-in-Aid for Scientific Research on Innovative Areas (22124003 to S.N.) and a Grant-in-Aid for Creative Scientific Research (15K06897, 18K06184 to T.B.) from the Ministry of Education, Culture, Sports, Science, and Technology of Japan.

Data availability
RNA-seq data have been deposited in the DDBJ Read Archive under accession numbers DRR287335 and DRR287334. Assembled transcriptome data have been deposited in DDBJ Transcriptome Shotgun Assembly (TSA) division under accession numbers ICRS01000001-ICRS01020314. Nucleotide sequences of *Gryllus* homologues of immune-related genes used in this study were deposited in GenBank under accession numbers LC422646-LC422679.

Peer review history
The peer review history is available online at https://journals.biologists.com/dev/article-lookup/doi/10.1242/dev.199916

References
Agaisse, H., Petersen, U.-M., Boutros, M., Mathey-Prevot, B. and Perrimon, N. (2003). Signaling role of hemocytes in *Drosophila* JAK/STAT-dependent response to septic injury. *Dev. Cell* **5**, 441-450. doi:10.1016/S1534-5807(03)00244-2

Agata, K. and Inoue, T. (2012). Survey of the differences between regenerative and non-regenerative animals. *Dev. Growth Differ.* **54**, 143-152. doi:10.1111/j.1440-169X.2011.01323.x

Agata, K., Saito, Y. and Nakajima, E. (2007). Unifying principles of regeneration I: epimorphosis versus morphallaxis. *Dev. Growth Differ.* **49**, 73-78. doi:10.1111/j.1440-169X.2007.00919.x

Anders, H.-J. and Schaefer, L. (2014). Beyond tissue injury — damage-associated molecular patterns, toll-like receptors, and Inflammasomes also drive regeneration and fibrosis. *J. Am. Soc. Nephrol.* **25**, 1387-1400. doi:10.1681/ASN.2014010117

Anthoney, N., Foldi, I. and Hidalgo, A. (2018). Toll and Toll-like receptor signalling in development. *Development* **145**, dev156018. doi:10.1242/dev.156018

Arbouzova, N. I. and Zeidler, M. P. (2006). JAK/STAT signalling in *Drosophila*: insights into conserved regulatory and cellular functions. *Development* **133**, 2605-2616. doi:10.1242/dev.02411

Bando, T., Mito, T., Maeda, Y., Nakamura, T., Ito, F., Watanabe, T., Ohuchi, H. and Noji, S. (2009). Regulation of leg size and shape by the Dachsous/Fat signalling pathway during regeneration. *Development* **136**, 2235-2245. doi:10.1242/dev.035204

Bando, T., Mito, T., Nakamura, T., Ohuchi, H. and Noji, S. (2011a). Regulation of leg size and shape: involvement of the Dachsous-fat signaling pathway. *Dev. Dyn.* **240**, 1028-1041. doi:10.1002/dvdy.22590

Bando, T., Hamada, Y., Kurita, K., Nakamura, T., Mito, T., Ohuchi, H. and Noji, S. (2011b). Lowfat, a mammalian Lix1 homologue, regulates leg size and growth under the Dachsous/Fat signaling pathway during tissue regeneration. *Dev. Dyn.* **240**, 1440-1453. doi:10.1002/dvdy.22647

Bando, T., Ishimaru, Y., Kida, T., Hamada, Y., Matsuoka, Y., Nakamura, T., Ohuchi, H., Noji, S. and Mito, T. (2013). Analysis of RNA-Seq data reveals involvement of JAK/STAT signalling during leg regeneration in the cricket Gryllus bimaculatus. *Development* **140**, 959-964. doi:10.1242/dev.084590

Bando, T., Hamada, Y. and Noji, S. (2017). Leg formation and regeneration. In *The Cricket as a Model Organism* (ed. H. W. Horch, T. Mito, A. Popadic, H. Ohuchi and S. Noji), pp. 31-48. Springer.

Benton, M. A., Pechmann, M., Frey, N., Stappert, D., Conrads, K. H., Chen, Y.-T., Stamataki, E., Pavlopoulos, A. and Roth, S. (2016). Toll genes have an ancestral role in axis elongation. *Curr. Biol.* **26**, 1609-1615. doi:10.1016/j.cub.2016.04.055

Bodó, K., Kellermayer, Z., László, Z., Boros, Á., Kokhanyuk, B., Németh, P. and Engelmann, P. (2021). Injury-induced innate immune response during segment regeneration of the earthworm, eisenia andrei. *Int. J. Mol. Sci.* **22**, 2363. doi:10.3390/ijms22052363

Browne, N., Heelan, M. and Kavanagh, K. (2013). An analysis of the structural and functional similarities of insect hemocytes and mammalian phagocytes. *Virulence* **4**, 597-603. doi:10.4161/viru.25906

Cattenoz, P. B., Sakr, R., Pavlidaki, A., Delaporte, C., Riba, A., Molina, N., Hariharan, N., Mukherjee, T. and Giangrande, A. (2020). Temporal specificity and heterogeneity of *Drosophila* immune cells. *EMBO J.* **39**, e104486. doi:10.15252/embj.2020104486

Cho, Y. and Cho, S. (2019). Hemocyte-hemocyte adhesion by granulocytes is associated with cellular immunity in the cricket, Gryllus bimaculatus. *Sci. Rep.* **9**, 18066. doi:10.1038/s41598-019-54484-5

Debuque, R. J., Nowoshilow, S., Chan, K. E., Rosenthal, N. A. and Godwin, J. W. (2021). Distinct toll-like receptor signaling in the salamander response to tissue damage. *Dev. Dyn.* Online Version of Record before inclusion in an is. doi:10.1002/dvdy.340

Erdman, L. K., Cosio, G., Helmers, A. J., Gowda, D. C., Grinstein, S. and Kain, K. C. (2009). CD36 and TLR interactions in inflammation and phagocytosis: implications for malaria. *J. Immunol.* **183**, 6452-6459. doi:10.4049/jimmunol.0901374

Evans, C. J., Hartenstein, V. and Banerjee, U. (2003). Thicker than blood: conserved mechanisms in *Drosophila* and vertebrate hematopoiesis. *Dev. Cell* **5**, 673-690. doi:10.1016/S1534-5807(03)00335-6

Franc, N. C., Dimarcq, J.-L., Lagueux, M., Hoffmann, J. and Ezekowitz, R. A. B. (1996). Croquemort, a novel *Drosophila* hemocyte/macrophage receptor that recognizes apoptotic cells. *Immunity* **4**, 431-443. doi:10.1016/S1074-7613(00)80410-0

Franc, N. C., Heitzler, P., Ezekowitz, R. A. B. and White, K. (1999). Requirement for croquemort in phagocytosis of apoptotic cells in *Drosophila*. *Science* **284**, 1991-1994. doi:10.1126/science.284.5422.1991

Godwin, J. W., Pinto, A. R. and Rosenthal, N. A. (2013). Macrophages are required for adult salamander limb regeneration. *Proc. Natl. Acad. Sci. USA* **110**, 9415-9420. doi:10.1073/pnas.1300290110

Guillou, A., Troha, K., Wang, H., Franc, N. C. and Buchon, N. (2016). The *Drosophila* CD36 homologue croquemort is required to maintain immune and gut homeostasis during development and aging. *PLoS Pathog.* **12**, e1005961. doi:10.1371/journal.ppat.1005961

Hamada, Y., Bando, T., Nakamura, T., Ishimaru, Y., Mito, T., Noji, S., Tomioka, K. and Ohuchi, H. (2015). Leg regeneration is epigenetically regulated by histone H3K27 methylation in the cricket Gryllus bimaculatus. *Development* **142**, 2916-2927. doi:10.1242/dev.122598

Hasegawa, T., Hall, C. J., Crosier, P. S., Abe, G., Kawakami, K., Kudo, A. and Kawakami, A. (2017). Transient inflammatory response mediated by interleukin-1β is required for proper regeneration in zebrafish fin fold. *eLife* **6**, e22716. doi:10.7554/eLife.22716

Hillyer, J. F. (2016). Insect immunology and hematopoiesis. *Dev. Comp. Immunol.* **58**, 102-118. doi:10.1016/j.dci.2015.12.006

Hu, X., Chen, J., Wang, L. and Ivashkiv, L. B. (2007). Crosstalk among Jak-STAT, Toll-like receptor, and ITAM-dependent pathways in macrophage activation. *J. Leukoc. Biol.* **82**, 237-243. doi:10.1189/jlb.1206763

Igaki, T. and Miura, M. (2014). The *Drosophila* TNF ortholog eiger: emerging physiological roles and evolution of the TNF system. *Semin. Immunol.* **26**, 267-274. doi:10.1016/j.smim.2014.05.003

Ishimaru, Y., Nakamura, T., Bando, T., Matsuoka, Y., Ohuchi, H., Noji, S. and Mito, T. (2015). Involvement of dachshund and Distal-less in distal pattern formation of the cricket leg during regeneration. *Sci. Rep.* **5**, 8387. doi:10.1038/srep08387

Ishimaru, Y., Bando, T., Ohuchi, H., Noji, S. and Mito, T. (2018). Bone morphogenetic protein signaling in distal patterning and intercalation during leg regeneration of the cricket, *Gryllus bimaculatus*. *Dev. Growth Differ.* **60**, 377-386. doi:10.1111/dgd.12560

Jiang, H., Tian, A. and Jiang, J. (2016). Intestinal stem cell response to injury: lessons from *Drosophila*. *Cell. Mol. Life Sci.* **73**, 3337-3349. doi:10.1007/s00018-016-2235-9

Kawai, T. and Akira, S. (2011). Toll-like receptors and their crosstalk with other innate receptors in infection and immunity. *Immunity* **34**, 637-650. doi:10.1016/j.immuni.2011.05.006

Krautz, R., Arefin, B. and Theopold, U. (2014). Damage signals in the insect immune response. *Front. Plant Sci.* **5**, 342. doi:10.3389/fpls.2014.00342

Kulkarni, O. P., Hartter, I., Mulay, S. R., Hagemann, J., Darisipudi, M. N., Kumar Vr, S., Romoli, S., Thomasova, D., Ryu, M., Kobold, S. et al. (2014). Toll-like receptor 4-induced IL-22 accelerates kidney regeneration. *J. Am. Soc. Nephrol.* **25**, 978-989. doi:10.1681/ASN.2013050528

Kumar, J. R., Smith, J. P., Kwon, H., Smith, R. C., Dionne, M. S. and Smith, R. C. (2021). Use of clodronate liposomes to deplete phagocytic immune cells in *Drosophila* melanogaster and Aedes aegypti. *Front. Cell Dev. Biol.* **9**, 627976.

Kux, K. and Pitsouli, C. (2014). Tissue communication in regenerative inflammatory signaling: lessons from the fly gut. *Front. Cell. Infect. Microbiol.* **4**, 49. doi:10.3389/fcimb.2014.00049

Kwon, H. and Smith, R. C. (2019). Chemical depletion of phagocytic immune cells in Anopheles gambiae reveals dual roles of mosquito hemocytes in anti-Plasmodium immunity. *Proc. Natl. Acad. Sci. USA* **116**, 14119-14128. doi:10.1073/pnas.1900147116

Lavine, M. D. and Strand, M. R. (2002). Insect hemocytes and their role in immunity. *Insect Biochem. Mol. Biol.* **32**, 1295-1309. doi:10.1016/S0965-1748(02)00092-9

Lemaitre, B. and Hoffmann, J. (2007). The host defense of *Drosophila melanogaster*. *Annu. Rev. Immunol.* **25**, 697-743. doi:10.1146/annurev.immunol.25.022106.141615

Lemaitre, B., Nicolas, E., Michaut, L., Reichhart, J.-M. and Hoffmann, J. A. (1996). The dorsoventral regulatory gene cassette spätzle/toll/cactus controls the potent antifungal response in *Drosophila* adults. *Cell* **86**, 973-983. doi:10.1016/S0092-8674(00)80172-5

Leulier, F. and Lemaitre, B. (2008). Toll-like receptors — taking an evolutionary approach. *Nat. Rev. Genet.* **9**, 165-178. doi:10.1038/nrg2303

Li, L., Yan, B., Shi, Y.-Q., Zhang, W.-Q. and Wen, Z.-L. (2012). Live imaging reveals differing roles of macrophages and neutrophils during zebrafish tail fin regeneration. *J. Biol. Chem.* **287**, 25353-25360. doi:10.1074/jbc.M112.349126

Li, G., Forero, M. G., Wentzell, J. S., Durmus, I., Wolf, R., Anthoney, N. C., Parker, M., Jiang, R., Hasenauer, J., Strausfeld, N. J. et al. (2020). A Toll-receptor map underlies structural brain plasticity. *eLife* **9**, e52743. doi:10.7554/eLife.52743

Lindsay, S. A. and Wasserman, S. A. (2014). Conventional and non-conventional *Drosophila* toll signaling. *Dev. Comp. Immunol.* **42**, 16-24. doi:10.1016/j.dci.2013.04.011

Liu, B., Zheng, Y., Yin, F., Yu, J., Silverman, N. and Pan, D. (2016). Toll receptor-mediated Hippo signaling controls innate immunity in Drosophila. *Cell* **164**, 406-419. doi:10.1016/j.cell.2015.12.029

McIlroy, G., Foldi, I., Aurikko, J., Wentzell, J. S., Lim, M. A., Fenton, J. C., Gay, N. J. and Hidalgo, A. (2013). Toll-6 and Toll-7 function as neurotrophin receptors in the *Drosophila* melanogaster CNS. *Nat. Neurosci.* **16**, 1248-1256. doi:10.1038/nn.3474

McLaughlin, C. N., Nechipurenko, I. V., Liu, N. and Broihier, H. T. (2016). A toll receptor–FoxO pathway represses Pavarotti/MKLP1 to promote microtubule dynamics in motoneurons. *J. Cell Biol.* **214**, 459-474. doi:10.1083/jcb.201601014

Ming, M., Obata, F., Kuranaga, E. and Miura, M. (2014). Persephone/Spätzle pathogen sensors mediate the activation of toll receptor signaling in response to endogenous danger signals in apoptosis-deficient *Drosophila*. *J. Biol. Chem.* **289**, 7558-7568. doi:10.1074/jbc.M113.543884

Mito, T. and Noji, S. (2008). The two-spotted cricket gryllus bimaculatus: an emerging model for developmental and regeneration studies. *Cold Spring Harb. Protoc.* **2008**, pdb.emo110. doi:10.1101/pdb.emo110

Mito, T., Inoue, Y., Kimura, S., Miyawaki, K., Niwa, N., Shinmyo, Y., Ohuchi, H. and Noji, S. (2002). Involvement of hedgehog, wingless, and dpp in the initiation of proximodistal axis formation during the regeneration of insect legs, a verification of the modified boundary model. *Mech. Dev.* **114**, 27-35. doi:10.1016/S0925-4773(02)00052-7

Miura, S., Takahashi, Y., Satoh, A. and Endo, T. (2015). Skeletal callus formation is a nerve-independent regenerative response to limb amputation in mice and xenopus. *Regeneration* **2**, 202-216. doi:10.1002/reg2.39

Morris, R., Kershaw, N. J. and Babon, J. J. (2018). The molecular details of cytokine signaling via the JAK/STAT pathway. *Protein Sci.*. **27**, 1984-2009. doi:10.1002/pro.3519

Moussian, B. and Roth, S. (2005). Dorsoventral axis formation in the *Drosophila* embryo—Shaping and transducing a morphogen gradient. *Curr. Biol.* **15**, R887-R899. doi:10.1016/j.cub.2005.10.026

Myllymäki, H., Valanne, S. and Rämet, M. (2014). The *Drosophila* Imd signaling pathway. *J. Immunol.* **192**, 3455-3462. doi:10.4049/jimmunol.1303309

Nakamura, T., Mito, T., Tanaka, Y., Bando, T., Ohuchi, H. and Noji, S. (2007). Involvement of canonical Wnt/Wingless signaling in the determination of the positional values within the leg segment of the cricket Gryllus bimaculatus. *Dev. Growth Differ.* **49**, 79-88. doi:10.1111/j.1440-169X.2007.00915.x

Nakamura, T., Mito, T., Bando, T., Ohuchi, H. and Noji, S. (2008a). Molecular and cellular basis of regeneration and tissue repair: dissecting insect leg regeneration through RNA interference. *Cell. Mol. Life Sci.* **65**, 64-72. doi:10.1007/s00018-007-7432-0

Nakamura, T., Mito, T., Miyawaki, K., Ohuchi, H. and Noji, S. (2008b). EGFR signaling is required for re-establishing the proximodistal axis during distal leg regeneration in the cricket Gryllus bimaculatus nymph. *Dev. Biol.* **319**, 46-55. doi:10.1016/j.ydbio.2008.04.002

Pandey, S., Kawai, T. and Akira, S. (2014). Microbial sensing by toll-like receptors and intracellular nucleic acid sensors. *Cold Spring Harb. Perspect .Biol.* **7**, a016246. doi:10.1101/cshperspect.a016246

Paré, A. C., Vichas, A., Fincher, C. T., Mirman, Z., Farrell, D. L., Mainieri, A. and Zallen, J. A. (2014). A positional Toll receptor code directs convergent extension in *Drosophila*. *Nature* **515**, 523-527. doi:10.1038/nature13953

Petrie, T. A., Strand, N. S., Tsung-Yang, C., Rabinowitz, J. S. and Moon, R. T. (2014). Macrophages modulate adult zebrafish tail fin regeneration. *Development* **141**, 2581-2591. doi:10.1242/dev.098459

Piccinini, A. M. and Midwood, K. S. (2010). DAMPening inflammation by modulating TLR signalling. *Mediators Inflamm.* **2010**, 1-21. doi:10.1155/2010/672395

Ramond, E., Dudzic, J. P. and Lemaitre, B. (2020). Comparative RNA-seq analyses of *Drosophila* plasmatocytes reveal gene specific signatures in response to clean injury and septic injury. *PLoS ONE* **15**, e0235294. doi:10.1371/journal.pone.0235294

Ribeiro, C. and Brehélin, M. (2006). Insect haemocytes: what type of cell is that? *J. Insect Physiol.* **52**, 417-429. doi:10.1016/j.jinsphys.2006.01.005

Satoh, T. and Akira, S. (2016). Toll-like receptor signaling and its inducible proteins. *Microbiol. Spectr.* **4**, 1-7. doi:10.1128/microbiolspec.MCHD-0040-2016

Schett, G., Dayer, J.-M. and Manger, B. (2016). Interleukin-1 function and role in rheumatic disease. *Nat. Rev. Rheumatol.* **12**, 14-24. doi:10.1038/nrrheum.2016.166

Seki, E., Park, E. J. and Fujimoto, J. (2011). Toll-like receptor signaling in liver regeneration, fibrosis and carcinogenesis. *Hepatol. Res.* **41**, 597-610. doi:10.1111/j.1872-034X.2011.00822.x

Shaukat, Z., Liu, D. and Gregory, S. (2015). Sterile inflammation in *Drosophila*. *Mediators Inflamm.* **2015**, 369286. doi:10.1155/2015/369286

Sokolova, I. I., Tokarev, I. S., Lozinskaia, I. L. and Glupov, V. V. (2000). A morphofunctional analysis of the hemocytes in the cricket Gryllus bimaculatus (Orthoptera: Gryllidae) normally and in acute microsporidiosis due to Nosema grylli. *Parazitologiia* **34**, 408-419.

Szatmary, Z. (2012). Molecular biology of toll-like receptors. *Gen. Physiol. Biophys.* **31**, 357-366. doi:10.4149/gpb_2012_048

Tamada, M., Shi, J., Bourdot, K. S., Supriyatno, S., Palmquist, K. H., Gutierrez-ruiz, O. L. and Zallen, J. A. (2021). Toll receptors remodel epithelia by directing planar-polarized Src and PI3K activity. *Dev. Cell* **56**, 1589-1602.e9. doi:10.1016/j.devcel.2021.04.012

Tsujioka, H., Kunieda, T., Katou, Y., Shirahige, K., Fukazawa, T. and Kubo, T. (2017). interleukin-11 induces and maintains progenitors of different cell lineages during Xenopus tadpole tail regeneration. *Nat. Commun.* **8**, 495. doi:10.1038/s41467-017-00594-5

Van Rooijen, N. , and Sanders, A. (1994). Liposome mediated depletion of macrophages: mechanism of action, preparation of liposomes and applications. *J. Immunol. Methods* **174**, 83-93. doi:10.1016/0022-1759(94)90012-4

Viljakainen, L. (2015). Evolutionary genetics of insect innate immunity. *Brief. Funct. Genomics* **14**, 407-412. doi:10.1093/bfgp/elv002

Vogg, M. C., Galliot, B. and Tsiairis, C. D. (2019). Model systems for regeneration: hydra. *Development* **146**, dev177212. doi:10.1242/dev.177212

Wang, L., Kounatidis, I. and Ligoxygakis, P. (2014). *Drosophila* as a model to study the role of blood cells in inflammation, innate immunity and cancer. *Front. Cell. Infect. Microbiol.* **3**, 113. doi:10.3389/fcimb.2013.00113

Wang, X., Xiang, L., Li, H., Chen, P., Feng, Y., Zhang, J., Yang, N., Li, F., Wang, Y., Zhang, Q. et al. (2015). The role of HMGB1 signaling pathway in the development and progression of hepatocellular carcinoma: a review. *Int. J. Mol. Sci.* **16**, 22527-22540. doi:10.3390/ijms160922527

Ward, A., Hong, W., Favaloro, V. and Luo, L. (2015). Toll receptors instruct axon and dendrite targeting and participate in synaptic partner matching in a *Drosophila* olfactory circuit. *Neuron* **85**, 1013-1028. doi:10.1016/j.neuron.2015.02.003

Westman, J., Grinstein, S. and Marques, P. E. (2020). Phagocytosis of necrotic debris at sites of injury and inflammation. *Front. Immunol.* **10**, 3030. doi:10.3389/fimmu.2019.03030

Williams, M. J. (2009). The c-src homologue Src64B is sufficient to activate the *Drosophila* cellular immune response. *J. Innate Immun.* **1**, 335-339. doi:10.1159/000191216

Xu, Q., Yu, X., Liu, J., Zhao, H., Wang, P., Hu, S., Chen, J., Zhang, W. and Hu, J. (2012). Ostrinia furnacalis integrin β1 may be involved in polymerization of actin to modulate spreading and encapsulation of plasmatocytes. *Dev .Comp. Immunol.* **37**, 438-445. doi:10.1016/j.dci.2012.02.003

Ylla, G., Nakamura, T., Itoh, T., Kajitani, R., Toyoda, A., Tomonari, S., Bando, T., Ishimaru, Y., Watanabe, T., Fuketa, M. et al. (2021). Insights into the genomic evolution of insects from cricket genomes. *Commun. Biol.* **4**, 733. doi:10.1038/s42003-021-02197-9

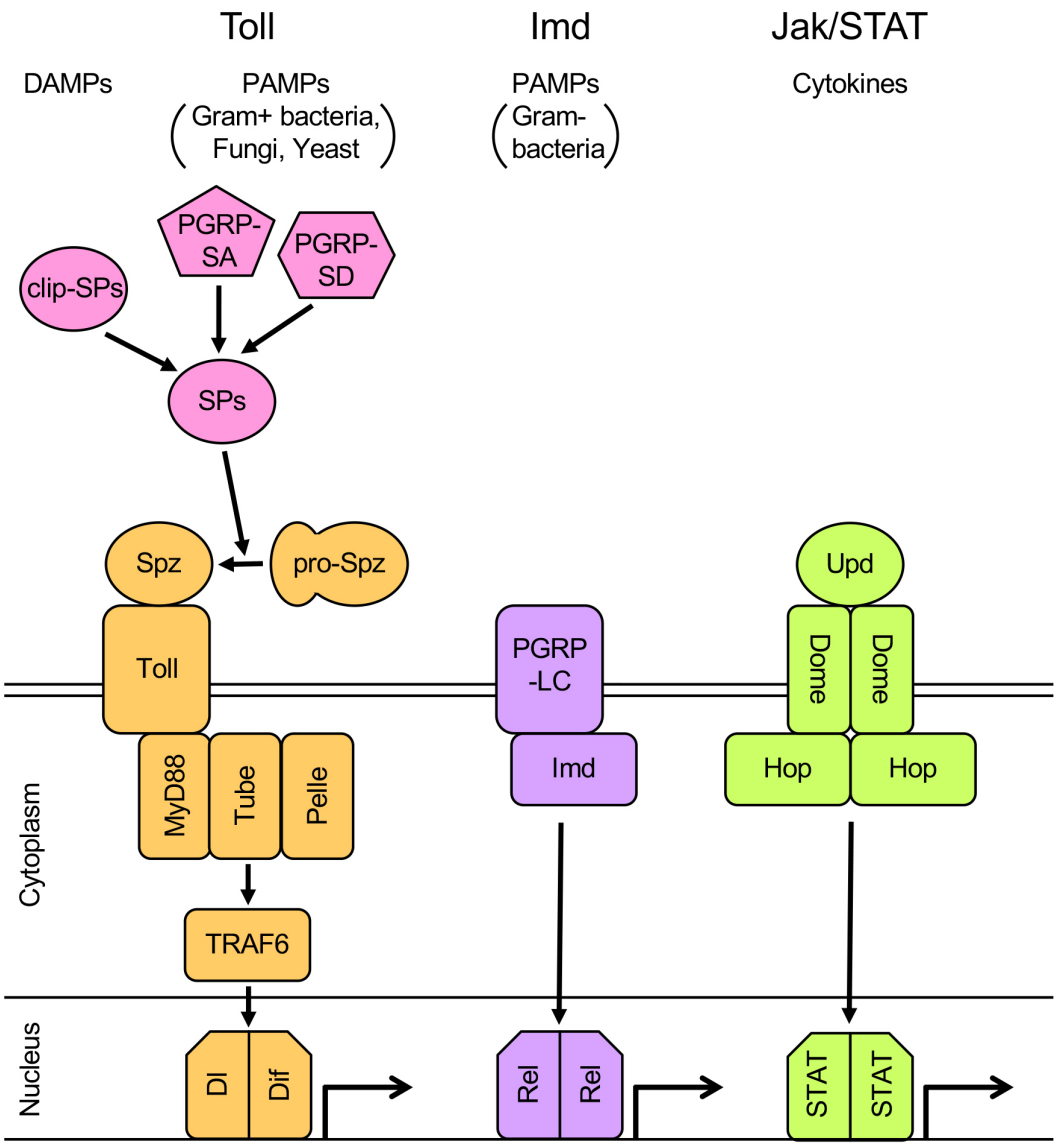

Fig. S1. Signalling pathways of insect immunity, after Hillyer (2016), Lindsay and Wasserman (2014) and Anthoney et al. (2018).
Schematic diagram of Toll, Imd, and JAK/STAT signalling pathways for insect immunity. Infectious pathogens, including gram-positive bacteria, fungi, and yeasts, are recognised by PGRP-SA and PGRP-SD, which activate clip-domain serine proteinases (clip-SPs) to catalyse pro-Spz to Spz. Matured Spz binds to Tolls and activates NF-κB transcription factors Dl and Dif via MyD88, Tube, Pelle, and TRAF6. DAMPs released from injured cells activate clip-SPs. Gram-negative bacteria are recognised by PGRP-LC via Imd and activate NF-κB transcription factor Rel. Insect cytokine Upd binds to interleukin receptor Dome and activates transcription factor STAT via Janus kinases Hop (Anthoney et al., 2018; Hillyer, 2016; Lindsay and Wasserman, 2014).
Abbreviations: JAK/STAT, Janus kinase/signal transducer and activator of transcription protein; NF-κB, nuclear factor kappa-B; Dl, dorsal; Dif, dorsal-related immunity factor; Dome, Domeless; MyD88, myeloid differentiation primary response 88; TRAF6, TNF receptor-associated factor 6; DAMPs, damage-associated molecular patterns; Psh, Persephone; PGRP, Peptidoglycan recognition protein; Spz, Spatzle; Hop, Hopscotch; Imd, Immune deficiency; Rel, Relish; Upd, Unpaired.

A

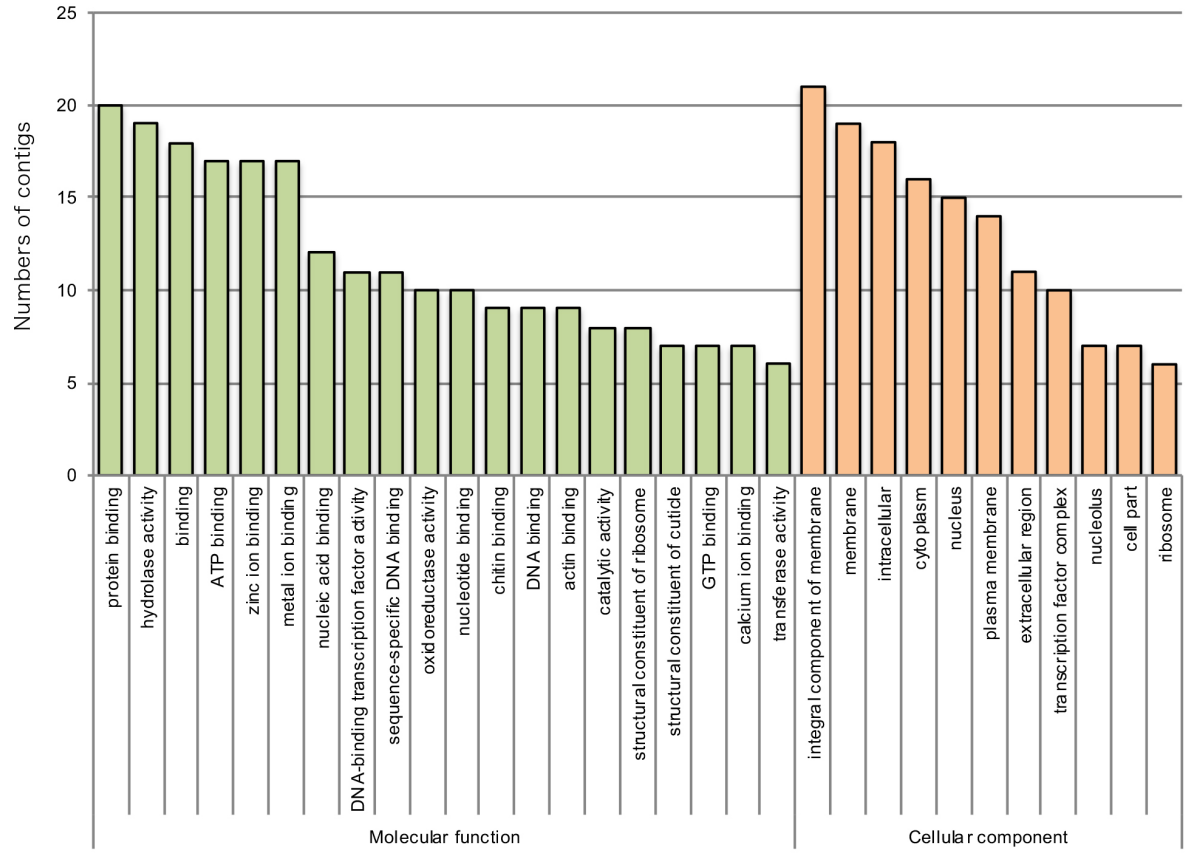

B

contig_ID	Sequence description	Length	0 hpa 595,425 reads in total # Reads	0 hpa RPKM	3 hpa 519,961 reads in total # Reads	3 hpa RPKM	RPKM Ratio 3h/0h
Transcription factors							
isotig04802	kayak	2,559	23	15.09	101	75.91	5.03
isotig11345	dna-binding protein d-ets-4	2,174	16	12.36	38	33.62	2.72
isotig06051	ets homologous factor-like	2,648	24	15.22	54	39.22	2.58
isotig16044	ap-1	1,030	38	61.96	72	134.44	2.17
VEGF signalling							
isotig15859	Platelet-derived and vascular endothelial growth factors	1,060	2	3.17	25	45.36	14.31
isotig13937	pvf3 cg34378-pd	1,380	3	3.65	17	23.69	6.49
isotig18768	vascular endothelial growth factor a-a-like	705	5	11.91	15	40.92	3.44
isotig03363	vascular endothelial growth factor receptor 1-like	6,760	29	7.2	71	20.2	2.81
isotig14929	vascular endothelial growth factor receptor 1 isoform x2	1,200	15	20.99	34	54.49	2.6
isotig14209	pdgf vegf receptor	1,325	7	8.87	13	18.87	2.13
IGF signalling							
isotig09133	tribbles homolog 2	4,891	136	46.7	254	99.88	2.14
FGF signaling							
isotig11083	dual specificity protein phosphatase mpk3-like	2,311	10	7.27	25	20.81	2.86
isotig11152	fgfr1 oncogene partner 2 homolog	2,269	10	7.4	21	17.8	2.41
TGF-β signalling							
isotig14196	transforming growth factor beta regulator 1	1,328	6	7.59	18	26.07	3.43
isotig03246	smad nuclear-interacting protein 1	2,945	17	9.69	30	19.59	2.02
Wnt signalling							
isotig12204	disheveled-associated activator of morphogenesis 2	1,823	10	9.21	34	35.87	3.89
Toll signalling							
isotig06664	Toll2-5	2,309	17	12.37	35	29.15	2.36
isotig12616	unc93-like	1,697	11	10.89	22	24.93	2.29
isotig05588	Relish	4,770	27	9.51	52	20.97	2.21
isotig09244	Toll8 (slit homolog 2)	4,522	43	15.97	82	34.87	2.18
isotig17867	Toll2-2	814	9	18.57	17	40.17	2.16
isotig11861	serine protease easter	1,956	45	38.64	79	77.68	2.01

Fig. S2. GO annotations of RNA-seq results.
(A) Graphs show 20 and 11 most frequently counted GO terms of molecular function and cellular components by annotations of the transcripts with upregulated expression in RLs. (B) Selected signalling pathway genes upregulated in RLs (3 hpa) compared with NLs (0 hpa). Note that contigs are assembled sequences of reads obtained from RLs and NLs, and isotigs are assembled sequences of contigs.

A

Gene name	Contig	Region (bp)
Toll	Contig34	815164 - 803187
Toll2-1	Contig175	1629363 - 1615808
Toll2-2	Contig590	2211452 - 2224860
Toll2-3	Contig7	597224 - 621200
Toll2-4	Contig79	4071160 - 4076220
Toll2-5	Contig175	2955568 - 2942763
Toll6-1	Contig285	4448827 - 4452034
Toll6-2	Contig330	781359 - 783951
Toll7	Contig330	7144339 - 7140837
Toll8	Contig285	7182752 - 7187271
Toll9	Contig121	18924776 - 18926973

B

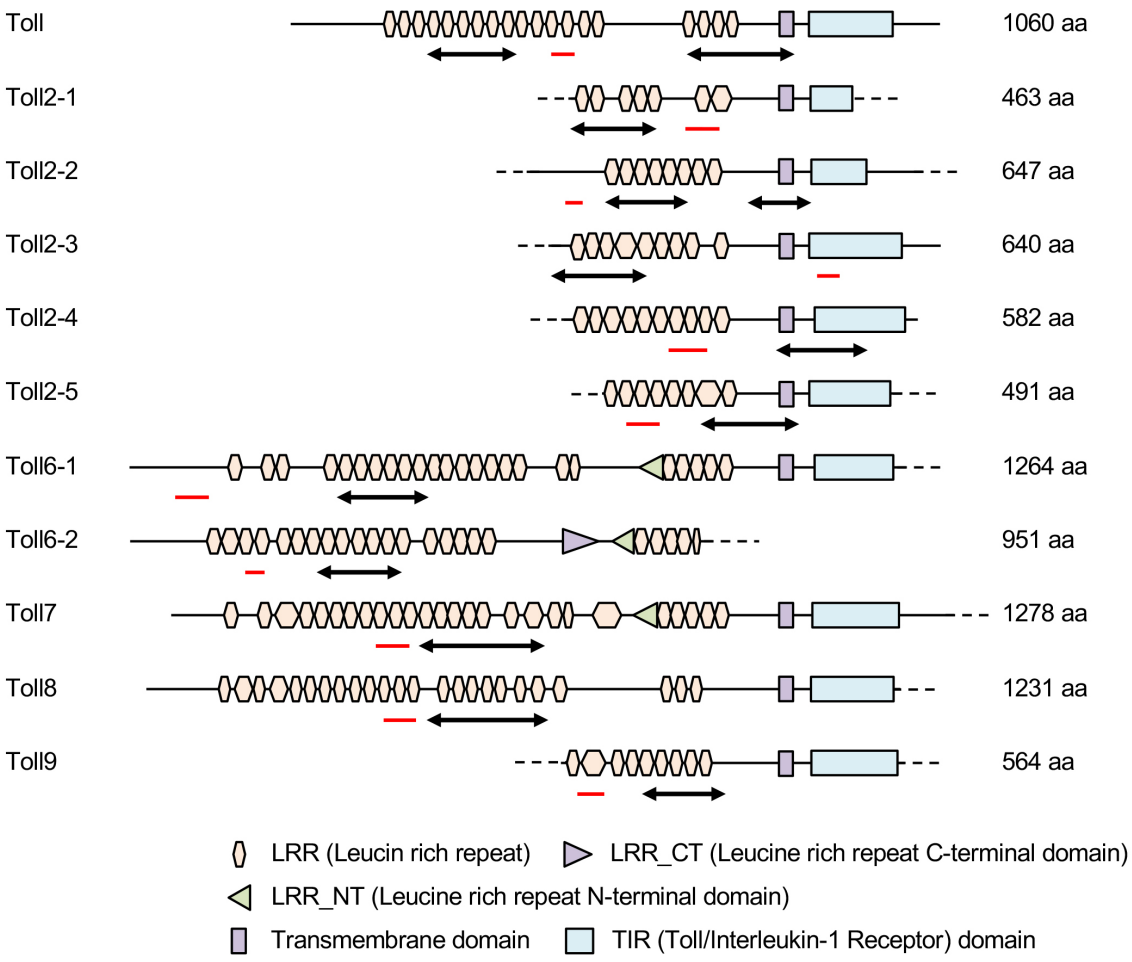

Fig. S3. Genomic loci of *Gryllus* Toll genes and their domain structures.

(A) Physical positions of *Gryllus* Toll genes spanning the genome contigs. Note that three pairs of Toll genes (*Toll2-1* and *Toll2-5*, *Toll6-1* and *Toll8*, and *Toll6-2* and *Toll7*) are located at the different regions of same contigs. (B) Schematic diagram of *Gryllus* Toll proteins is shown. Domains were predicted by Protein BLAST at NCBI web BLAST (https://blast.ncbi.nlm.nih.gov/Blast.cgi) and SMART website (http://smart.embl-heidelberg.de/). Dotted lines indicate regions that we have not cloned. Double-headed arrows and red lines indicate regions for RNAi and qPCR, respectively. To verify the specificity of RNAi against *Toll* or *Toll2-2*, we compared the phenotype using dsRNAs corresponding to two independent regions of each gene. The phenotypic effects by RNAi against *Toll(5')*, which correspond to an extracellular LRR region, and *Toll(3')*, which corresponds to an extracellular region and transmembrane domain were not significantly different ($p>0.05$, Fisher's exact test) (see Fig. S4B). The similar results were obtained for *Toll2-2*^{RNAi}. We therefore used the *Toll(5')* and *Toll2-2(5')* fragments for all subsequent analyses.

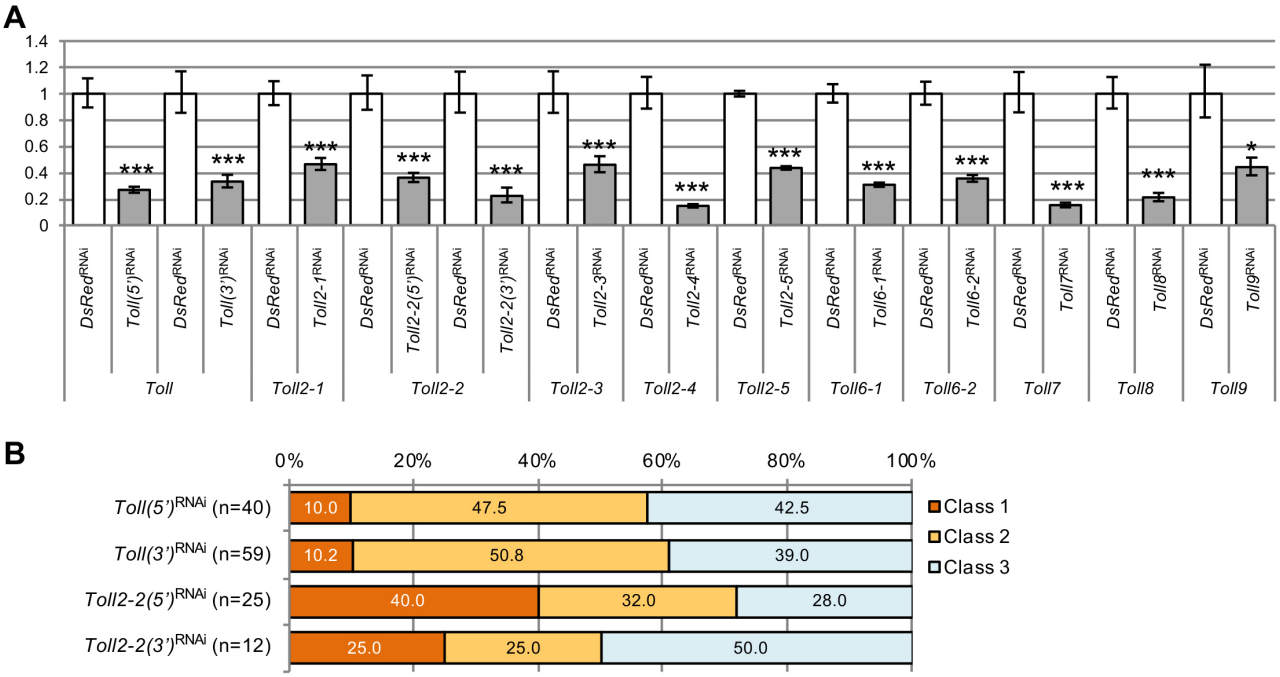

Fig. S4. Efficiencies of RNAi for *Gryllus* Toll genes.

(A) RNAi efficiencies to endogenous on-target genes, revealed by qPCR. Two independent regions of *Toll* (*Toll(5')* and *Toll(3')*) and *Toll2-2* (*Toll2-2(5')* and *Toll2-2(3')*) were used for RNAi experiments to observe phenotype reproducibility. The y-axis indicates normalized expression of *Gryllus* Toll genes in the *DsRed*^{RNAi} samples and relative expression levels in the RNAi samples against the corresponding Toll genes. Asterisks indicate significance between *DsRed*^{RNAi} and RNAi against Toll genes (*$p < 0.05$, ***$p < 0.001$ by Student's t-test). (B) Graph shows the percentage of class 1, class 2, and class 3 phenotypes obtained by RNAi against two independent regions of *Toll* and *Toll2-2* genes. Numbers of RNAi-treated individuals are shown by *n*. The phenotype ratios of *Toll(5')*^{RNAi} and *Toll(3')*^{RNAi} were similar ($p = 0.954747$, Fisher's exact test) and those of *Toll2-2(5')*^{RNAi} and *Toll2-2(3')*^{RNAi} were also similar ($p=0.462691$, Fisher's exact test).

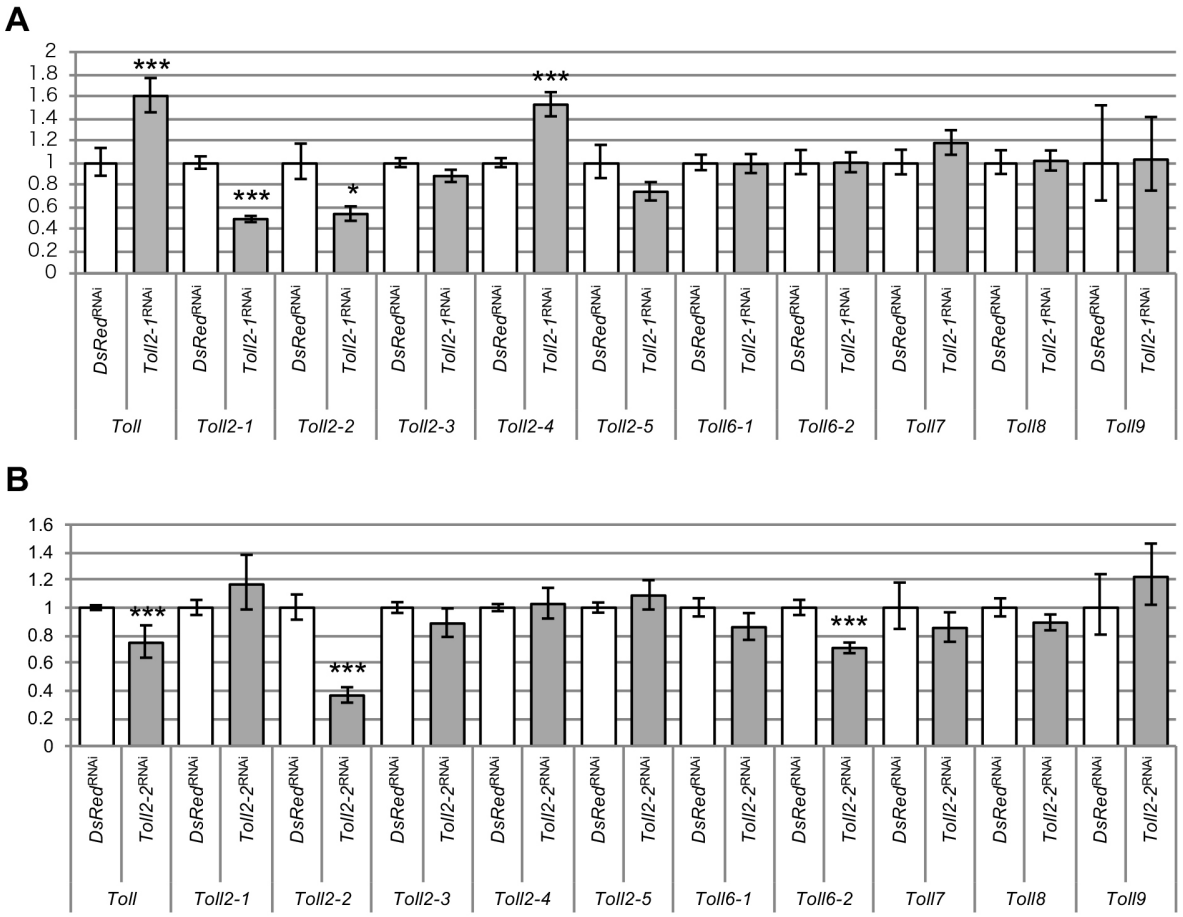

Fig. S5. Efficiencies of RNAi for *Toll2-1* and *Toll2-2* genes.

(A,B) RNAi efficiencies to on-target and off-target genes by *Toll2-1*^{RNAi} (A) and *Toll2-2*^{RNAi} (B). The y-axes indicate normalized expression of *Gryllus* Toll genes in the *DsRed*^{RNAi} samples and relative expression levels in the RNAi samples against the corresponding Toll genes. Asterisks indicate significance between *DsRed*^{RNAi} and RNAi against each Toll gene (*$p < 0.05$, ***$p < 0.001$ by Student's t-test). (C) The nucleotide sequence homology between the dsRNA region of *Toll2-1* and the most homologous region of *Toll2-2*. The homology score was 49.46% between them. We could not find the homologous region that spans more than 21 bp, which would work as siRNA to inhibit *Toll2-2* expression, when we injected *Toll2-1* dsRNA.

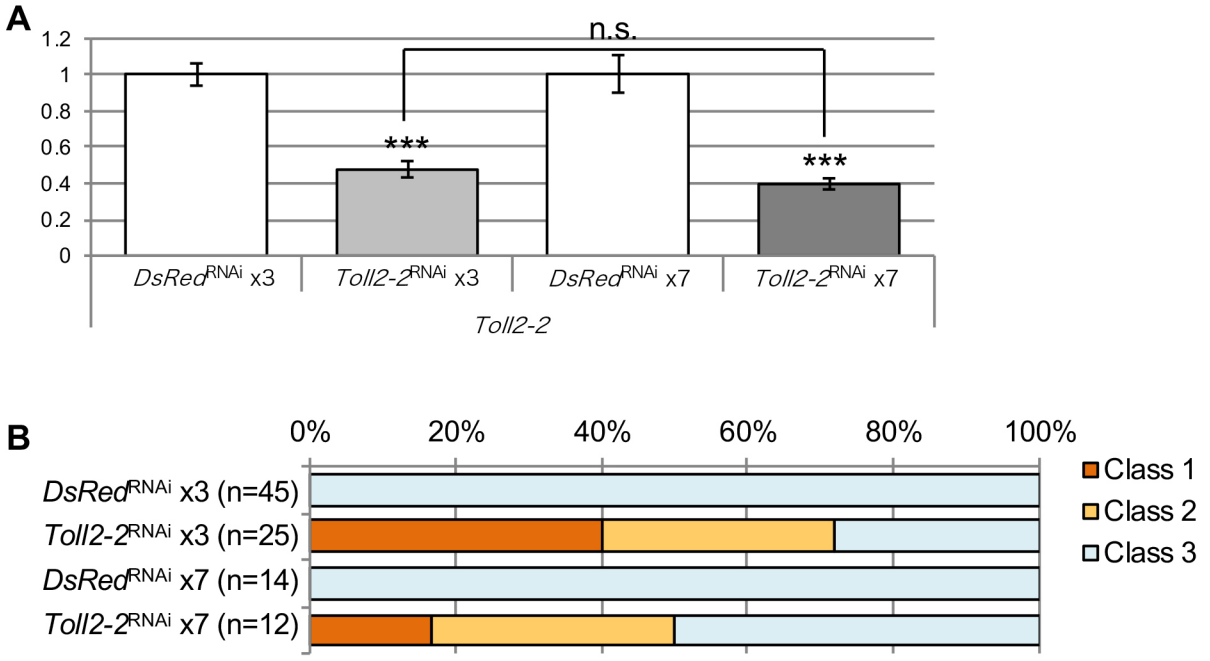

Fig. S6. RNAi efficiency and phenotype ratio of *Toll2-2*^{RNAi} in different dsRNA dose.

(A) Relative expression levels of *Toll2-2* after *Toll2-2*^{RNAi} x3 (207 nL dsRNA injection) or *Toll2-2*^{RNAi} x7 (483 nL dsRNA injection) to see RNAi efficiencies. The y-axis indicates normalized expression of *Toll2-2* in the *DsRed*^{RNAi} samples and relative expression levels in the *Toll2-2*^{RNAi} samples. 207 nL or 483 nL of *DsRed* dsRNA were injected into control nymphs. Relative expression levels of *Toll2-2* in *Toll2-2*^{RNAi} x3 and *Toll2-2*^{RNAi} x7 were significantly reduced compared with respective control experiments (***$p < 0.001$ by Student's t-test), but reduction of *Toll2-2* expression by *Toll2-2*^{RNAi} x7 was not significant to that by *Toll2-2*^{RNAi} x7 (n.s.; not significant). (B) Phenotypic ratios of RNAi by *Toll2-2*^{RNAi} x3 or *Toll2-2*^{RNAi} x7. Ratios of class 1 and class 2 were not significantly changed by *Toll2-2*^{RNAi} x7 compared with *Toll2-2*^{RNAi} x3 ($p>0.05$, Fisher's exact test).

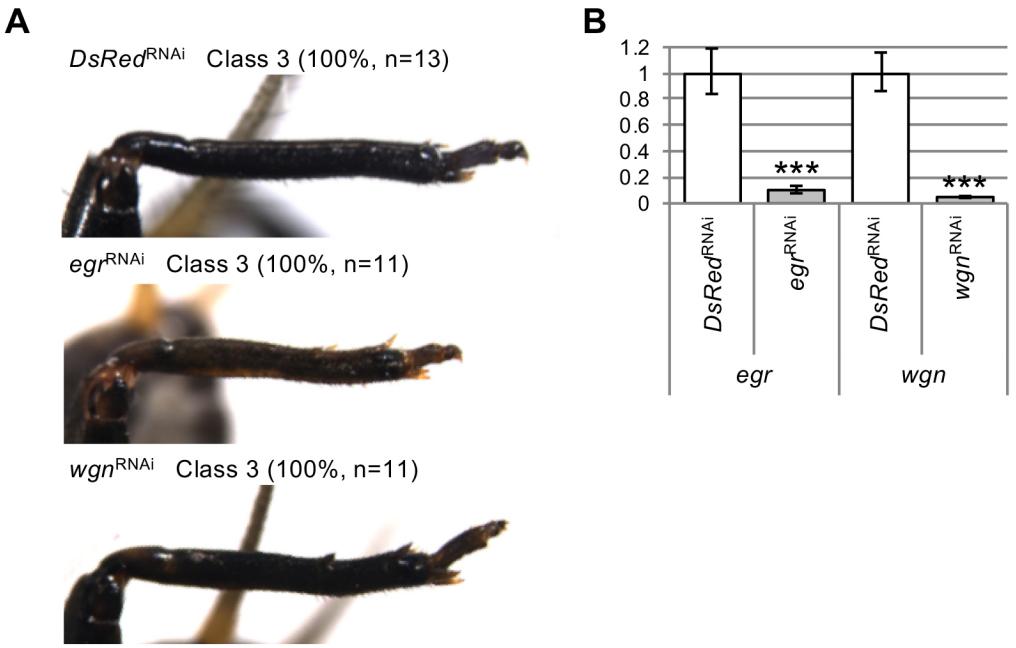

Fig. S7. Phenotypes of RNAi for *egr* and *wgn*.

Typical morphology of regenerating legs of *DsRed*^{RNAi}, *egr*^{RNAi}, or *wgn*^{RNAi} crickets at the fifth instar. Note that these RNAi crickets regenerated the lost part normally, and no RNAi crickets showed class 1 or 2 phenotypes. (B) Efficiency of RNAi against *egr* and *wgn*. The y-axis indicates normalized expression of *egr* and *wgn* in the *DsRed*^{RNAi} samples and relative expression levels in the *egr*^{RNAi} and *wgn*^{RNAi} samples. Asterisks indicate significance between *DsRed*^{RNAi} and RNAi against *egr* or *wgn* (***$p < 0.001$ by Student's t-test).

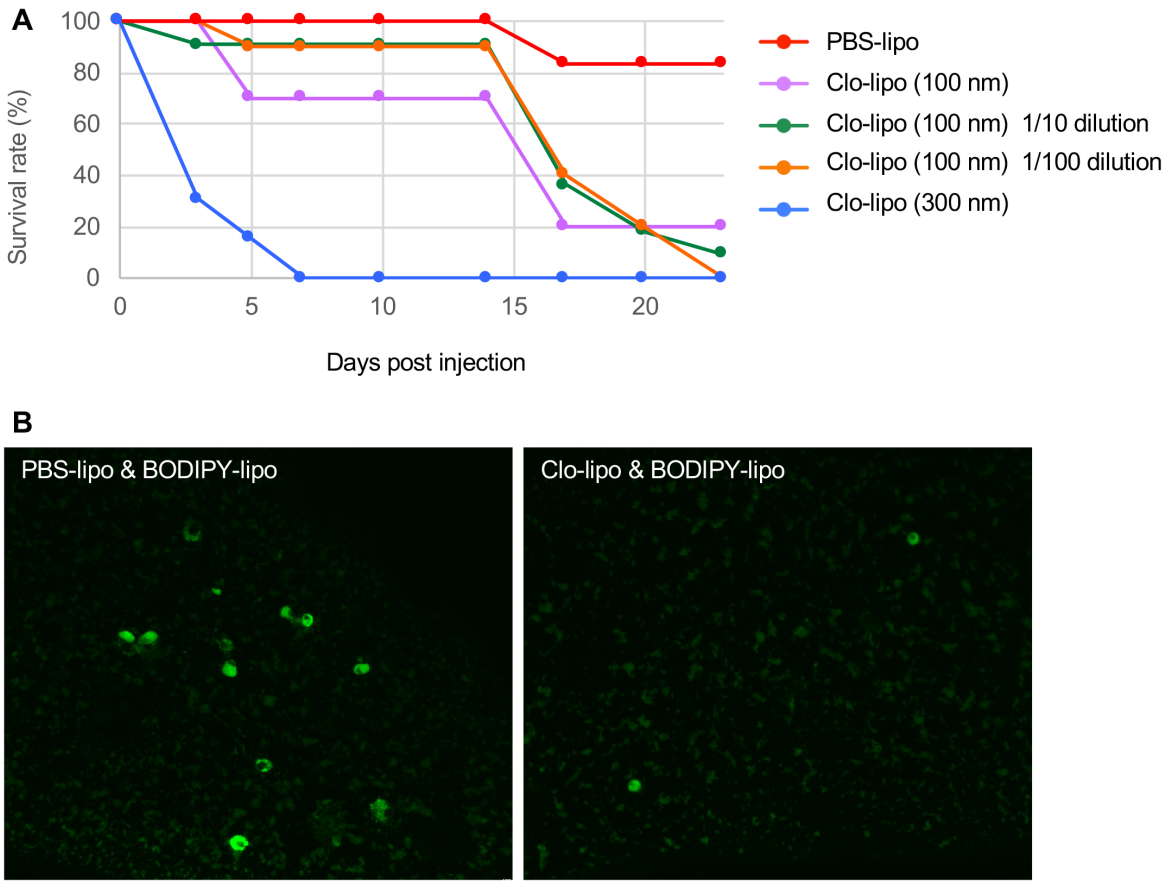

Fig. S8. Effects of plasmatocyte depletion.

(A) Survival curve of PBS-lipo, Clo-lipo (100 nm) or Clo-lipo (300 nm) injected cricket nymphs. The mean lifespan of Clo-lipo (100 nm) injected crickets was 15 days, which was longer than that of Clo-lipo (300 nm) injected crickets (2.5 days). The short lifespan of Clo-lipo (300 nm) injected crickets was an obstacle to observing regeneration processes. Thus, we used Clo-lipo (100 nm) to deplete the plasmatocytes in this study. PBS was used as the diluent. (B) Plasmatocytes in the haemolymph were visualised by BODIPY-lipo incorporation in the PBS-lipo injected or Clo-lipo injected crickets.

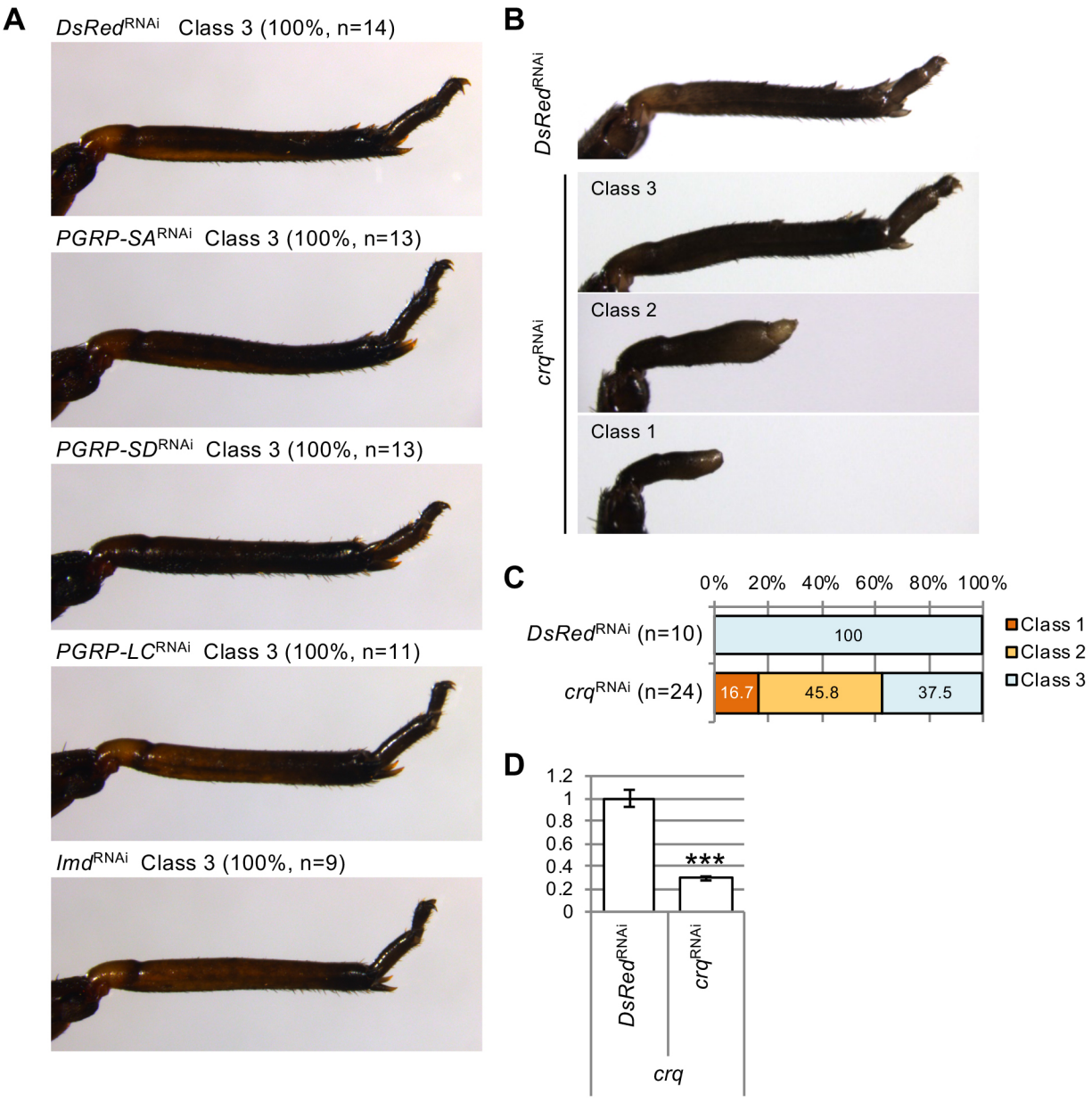

Fig. S9. Phenotypes after RNAi to PAMPs and cellular debris recognising molecule genes.
(A) Typical morphology of regenerating legs of *DsRed*^{RNAi}, *PGRP-SA*^{RNAi}, *PGRP-SD*^{RNAi}, *PGRP-LC*^{RNAi}, or *imd*^{RNAi} crickets at fifth instar. Note that all of *PGRP-SA*^{RNAi}, *PGRP-SD*^{RNAi}, *PGRP-LC*^{RNAi}, or *imd*^{RNAi} crickets show normal leg regeneration. (B-D) Phenotypes and efficiency of RNAi for *crq*. (B) Morphology of regenerating legs of *DsRed*^{RNAi} and *crq*^{RNAi} crickets at fifth instar. (C-D) Phenotype ratio (C) and efficiencies (D) of *DsRed*^{RNAi} and *crq*^{RNAi}. *crq*^{RNAi} significantly decreased the amount of *crq* transcripts to 29.4% in regenerating legs at 48 hpa. The y-axis indicates normalized expression of *crq* in the *DsRed*^{RNAi} and a relative expression level in the *crq*^{RNAi}. Asterisks indicate significance between *DsRed*^{RNAi} and *crq*^{RNAi} samples (***$p < 0.001$ by Student's t-test).

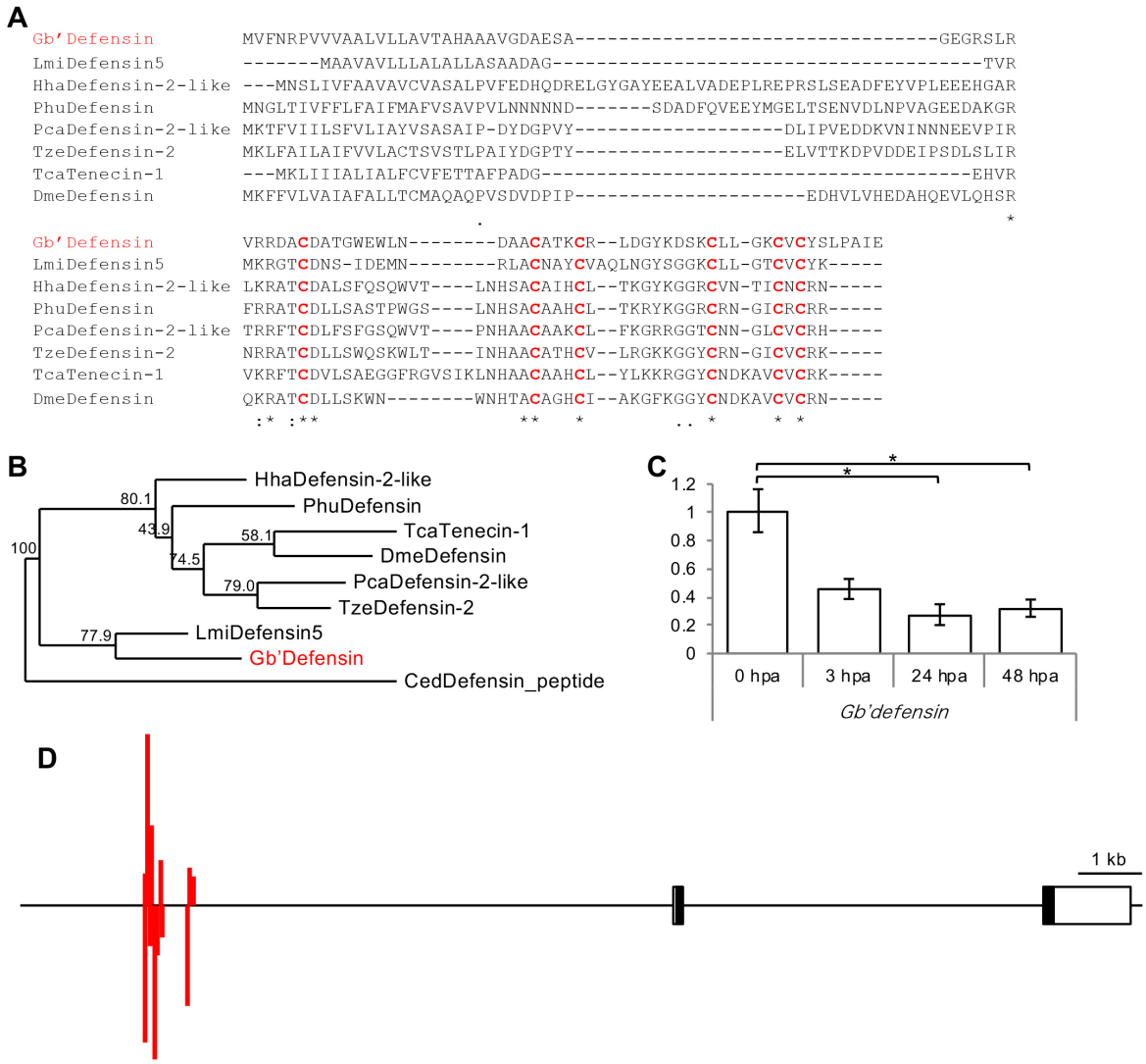

Fig. S10. Amino acid homology, phylogenetic tree and expression of *Gb' defensin*.
The *Gryllus bimaculatus* genome contains a single *defensin* gene. (A) *Gb' defensin* encodes 84 amino acids, with six evolutionarily conserved cysteine residues, shown in red. The N-terminal region of *Gb'* Defensin has diverged from the Defensins of other insects, but the C-terminal domain contains six evolutionarily conserved cysteine residues. (B) The phylogenetic tree indicates that *Gb'* Defensin is evolutionarily close to the grasshopper *Locusta migratoris* Defensin. *Centruroides edwardsii* was selected as the outgroup. (C) Temporal expression changes of *Gb' defensin* during leg regeneration, as revealed by qPCR. The y-axes indicate normalized expression at the 0 hpa and relative expression levels at 3, 24 and 48 hpa. Asterisks indicate significance of expression changes (*$p < 0.05$) by Tukey's test. (D) Spatial distribution of NF-κB binding sites (dl(var.2)) in the upstream region of *Gb' defensin*, by using Cister website (http://www.ijdb.ehu.es/web/), are indicated by red lines. Black boxes and white boxes represent coding and non-coding regions, respectively. Red bar lengths indicate probabilities. Gb, *Gryllus bimaculatus*, Lmi, *Locusta migratoria*, Tze, *Trachymyrmex zeteki*, Pca, *Polistes canadensis*, Hha, *Halyomorpha halys*, Phu, *Pediculus humanus*, Tca, *Tribolium castaneum*, Dme, *Drosophila melanogaster*. CedDefensin_peptide (*Centruroides edwardsii*) was selected as an outgroup.

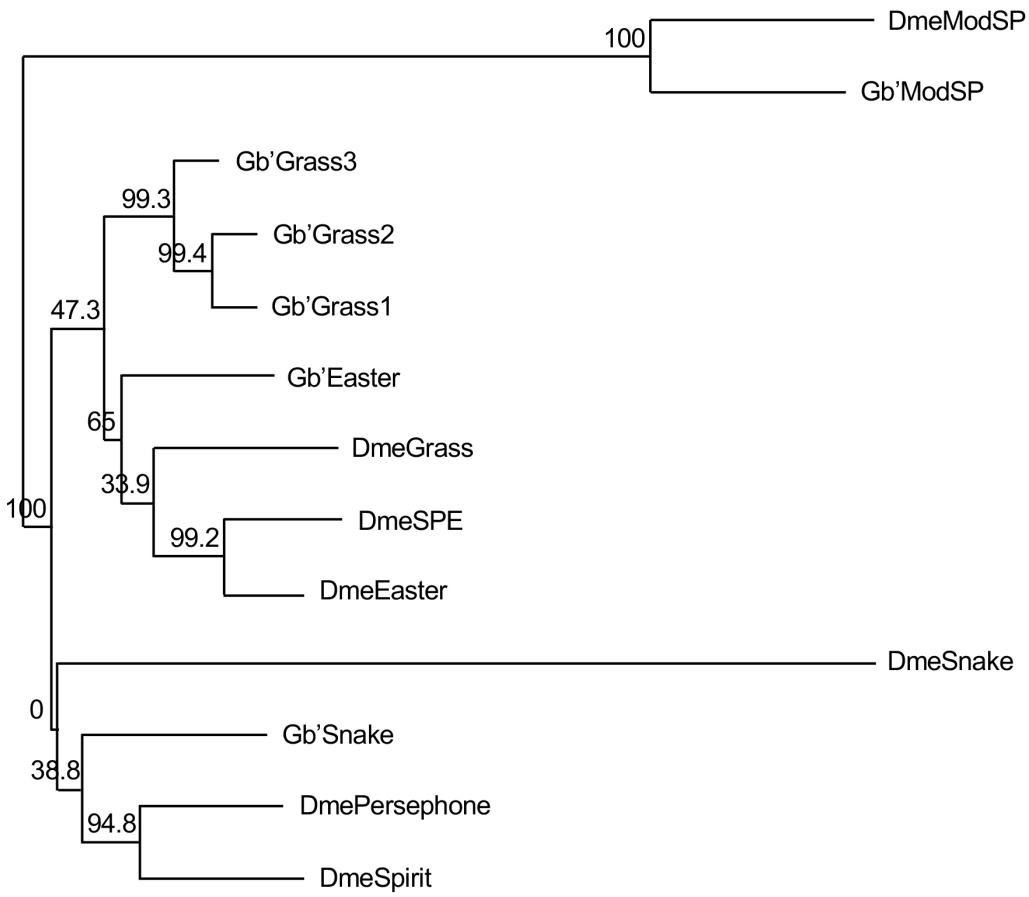

Fig. S11. Phylogenetic tree of Toll signalling-related proteinases

Phylogenetic tree of Toll signalling-related serine proteinases in *Gryllus* and *Drosophila*. *Gryllus* genome contains ModSP, Easter, and Snake homologues, and three Grass paralogues (Grass1, Grass2 and Grass3). We could not find *Drosophila* SPE and Persephone homologues in the *Gryllus* genome.

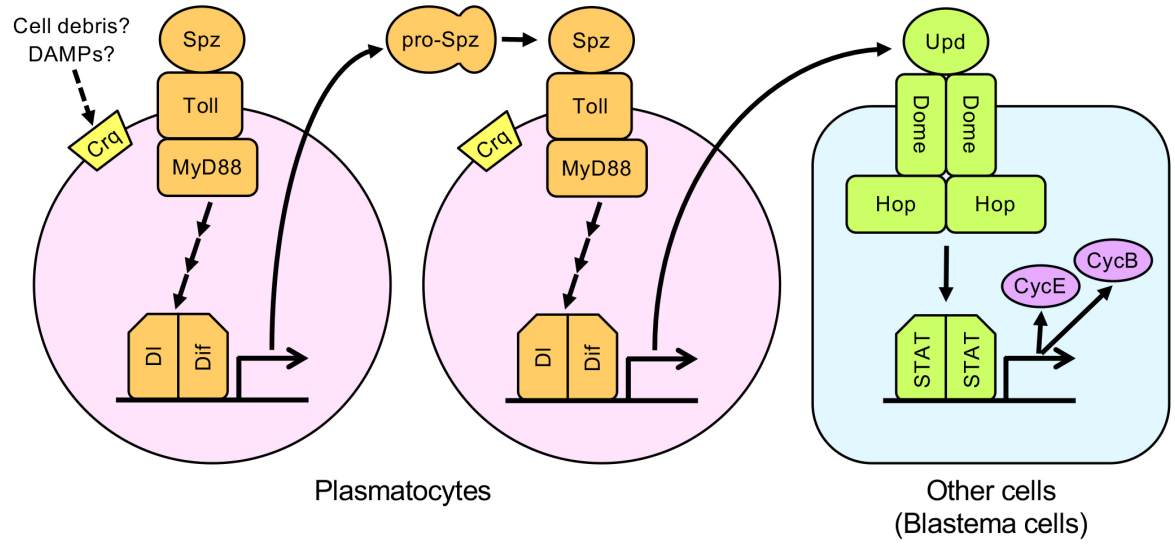

Fig. S12. Roles of Toll signalling during leg regeneration.

Schematic representation of Toll signalling during regeneration. In the plasmatocytes, Crq, and probably also Toll2-2, recognises apoptotic cells and cell debris caused by amputation and activates Toll signalling. Activated Toll signalling induces the *spz/spz2* expression that activates Toll signalling in surrounding plasmatocytes to lead accumulation of plasmatocytes in regenerating leg, and *upd* expression that activates JAK/STAT signalling in other cells including blastema cells mediated by the expression of Cyclin E and Cyclin B, which promote cell proliferation during regeneration.

Table S1. Comparison of expressed contigs between regenerating legs (3 hpa) and non-regenerating legs (0 hpa). Comparison of RPKM values of contigs between regenerating legs and non-regenerating legs. Contigs are ordered by RPKM values of regenerating legs.

Click here to download Table S1

Table S2. Blast results of contigs only expressed in or upregulated in the regenerating legs. Blast annotations are listed. Contigs are ordered by ratios of RPKM values of between regenerating legs and non-regenerating legs.

Click here to download Table S2

Table S3. Primer sequences for gene cloning

Targeted gene	Forward primer (5' -> 3')	Reverse primer (5' -> 3')	Amplicon size
spz	CATGAATGGAGAGAAATCATTA	CATAACAAACACAACACGATG	302
spz2	GTATCGCACTATAATCCTGACGAAT	GTGTGATTTGACACACACAACAGT	436
Toll(5)	GGAAACAAAATCTCAAATCTAACAAAA	AAGCTCTTTTAGATACTCTGTGTCTCG	426
Toll(3)	TCAAGAATTACTTAATCCAACATTTCC	ACCAAACTTTGACTTCATTTTGATAAC	524
Toll2-1	AATTATTGAATACCTGGATCTATCACG	TTTGTTTTGAGACATGTTCAGTACTTC	520
Toll2-2(5)	ATAGGATTGAAATTGCTGATTATTACG	AGTTTGTTTAGACCTTTAAATGCAATG	434
Toll2-2(3)	ACAACACTGGTTAGACGTCACAAAA	AAGCCTTTCTTTCAGTCTCCTTCTC	302
Toll2-3	CAACTTCCTACTGGGCTACCTG	GGATATGTTGCAAGTACTCACGTC	472
Toll2-4	CTTACATTATAGTAGGCGTGGTCCTC	AAAGAATAAACTGTAATGTTCCGCTAA	449
Toll2-5	GTTGAAATTACAGAACAATCTGTAGCA	ATGTTTTGAGAGATAAAAGAACCAAGA	545
Toll6-1	GAAGTTTTCGATCTGTCGAATAATAAA	AACTAAGTACGTACAAACCGTTGAGAG	445
Toll6-2	AGATATCAAAGAAGTGTACCTGCAGAA	AGGTCTTTGATTCGATTGTTAGAGAG	411
Toll7	ACGATTAGCAATAATCTTCTCATTAGC	GTAGTCGAACCACACTAAATGGTTATT	462
Toll8	AATCAGTTCCTAGATGTTCCTGAAGTA	AAGTATACGACTGCACCTTGTTGAT	598
Toll9	ACAATAATTTAAGAGAGCATTTAGGCA	AAAGAACTCAATCATTGGACAACTATC	407
MyD88	CAGTACCGAATTTATATGACATTCCTC	CAACACATCATCTCTCGTTAATATTTC	404
tube	AAAAGATTAAAGAATGATGCTGTCAGT	TAAGCTGATGTTCCAAATACTGTAGTG	431
pelle	CGGCATGATAATATACTTCCTTTGTAT	ACTTTTGTAGACAACTGTTTGTTCCTT	389
TRAF6	AAATGAAGAGACTGACTTATTTCCAGA	TATATCACTCACAGTCCAAACAAGAAC	559
dl	AGCCAGTAGTACTCCAGATAACAAGAC	AGAAGCGAACTTGGATATCTTCTTTAG	548
Dif	TCATCATCATCAATGAGTAATAAAAGC	TCCTTCTAAAAAGACTTGGAAACATAA	486
Rel	ACAATGAATAGAGAAGAGCCATTTTTA	CAGTCAAAGCACTTTTCATATTGTTTA	625
upd	GAGAACTTCAAAGAGAAATATGTCCAG	CCATTCATGTAGTCACGGTAGATTAG	455
egr	ACTTCGAAGGTAACGGAAAGC	CAGTGTGACCCAGTTTGACAAG	414
wgn	ACTAAGTTTGATGGTACCAGAACTCG	TTTATTGTTTTAACAAACATATTTACTCCT	322
Imd	GATCCTCCCAGAGTTGAAATACAC	CAGTAACATCTGATACACCACCTCTTT	537
PGRP-SA	AGAATCGATTATATGGTGATTCCACT	GGATCTCCTGGAAGAGTGCTAGT	424
PGRP-SD	GTCTGGTGGAAATATGAATCAGATAAT	CCTTCTTCTAAGAACTTCTGACACACT	418
PGRP-LC	TTTGGTAACAAAACTTTTTATAATGGC	ATGATAACATATGGCACTGGTGTAGTA	566
crq	TATGTTACAAAGACAGTGAAGGAGTTG	AGTGGTGTTAAGTATGATGAATTAGCC	566

Table S4. Primer sequences for qPCR

Targeted gene	Forward primer (5' -> 3')	Reverse primer (5' -> 3')	Amplicon size
actin	TTGACAATGGATCCGGAATGT	AAAACTGCCCTGGGTGCAT	64
spz	GCCAATTCAAACCACGCTTC	CATCCACGCCTCCTTCACA	81
spz2	GATACCCCGACCGTCGATAC	GCAGCAGGGTGGTGTAGAGA	81
Toll	ATCACTCATCTCCTCCTACCC	AACCCAGCTAATTCACCGTTT	134
Toll2-1	CGGAAGTGGGTGATGCGT	GATGACCTTCCTGCTGTGCT	147
Toll2-2	ATTCGATGATGGACTCTTTGTAGGA	CGTGGAGATGAAAAGCGGTAAAG	121
Toll2-3	GCCCTCCCACCAAACCTC	TGACCATCTCAGATAAACATCACACA	145
Toll2-4	TGGAACCGTGGATTGAAGAGG	CAACATGACTGGGCTGAGGT	101
Toll2-5	TCCAAGACACTCATCACATCACT	TTGAATTGAAGGCAGTTGACACTC	105
Toll6-1	ACACCACCAACTTCAGCGT	GCGGGTCAGGTGGTAGAAG	119
Toll6-2	CCGCGATGACCATGGAGTT	GGTTGCGCGTGAGGTTG	150
Toll7	CAGAACTCCATCGGCTACATC	GTTAAACATCAACGGCCCTATTTC	111
Toll8	AACACCTTTGCCTCTCTTTACAATC	AATGCTTCGGATGTTGTTGTTATCT	138
Toll9	GCCACTCCAAACCTTCAAACA	ACTTTTGTTCCTTCTAATGTTCCTCA	117
cycE	AGCAACAGGAGGAAGGAGCA	CCAGGGCAGCATAAGGAAAC	144
cycB	CCCAGGTGGAGGTCAAGAGA	GGAAATTCGTGGTCGGAAAA	132
upd	AGGTGCAAGTGCTGATGGTG	GCGACGTGCTGTTGTTTTGT	99
dome	CAGTGACGGAAGTTACCAATTCAT	TGTAAAAGCGAAGTACACCATTCATT	81
hop	CCTCCTTCAGAATATGATCGTTCA	ACGATCCCAGGCCAGAAAA	91
STAT	TGGGCCAAGGGTTATCACTAGT	CCTGTGTGCGTCTGCGTAAA	81
egr	GATTCATACATATTCAAAGCTCCTACAATC	ACTGTTGTACCATGAAGAAAGCAA	100
wgn	TGAACTGCTAATTTGATGTTTACGAATG	GCCATTAACCACGCACATGAA	119
crq	ATTGCTGGTCTCGGTGCTTT	GTTCGTGGTCCTGGGTCTCT	88
Gcm	CGGTCTGTGTTGTGTCCTTTG	ATGCTGGAACTGGGGATTGT	150

References

Anthoney, N., Foldi, I. and Hidalgo, A. (2018). Toll and Toll-like receptor signalling in development. *Development* **145**, dev156018.

Hillyer, J. F. (2016). Insect immunology and hematopoiesis. *Dev Comp Immunol* **58**, 102–118.

Lindsay, S. A. and Wasserman, S. A. (2014). Conventional and non-conventional Drosophila Toll signaling. *Dev. Comp. Immunol.* **42**, 16–24.